UMTRI-2015-21

A Pilot Study of Law Enforcement Officer (LEO) Anthropometry with Applications to Vehicle Design for Safety and Accommodation

Monica L.H. Jones
Sheila M. Ebert
Matthew P. Reed

June 2015

UMTRI-2015-21

A Pilot Study of Law Enforcement Officer (LEO) Anthropometry with Applications to Vehicle Design for Safety and Accommodation

Monica L.H. Jones
Sheila M. Ebert
Matthew P. Reed

The University of Michigan
Transportation Research Institute
Ann Arbor, MI 48109-2150
U.S.A.

June 2015

Technical Report Documentation Page

1. Report No.	2. Government Accession No.	3. Recipient's Catalog No.
UMTRI-2015-21		

4. Title and Subtitle	5. Report Date
A Pilot Study of Law Enforcement Officer (LEO) Anthropometry with Applications to Vehicle Design for Safety and Accommodation	June 2015
	6. Performing Organization Code XXXXXX

7. Author(s)	8. Performing Organization Report No.
Jones, M.L.H, Ebert, S.M., and M.P. Reed	UMTRI-2015-21

9. Performing Organization Name and Address	10. Work Unit no. (TRAIS)
The University of Michigan Transportation Research Institute 2901 Baxter Road Ann Arbor, Michigan 48109-2150 U.S.A.	11. Contract or Grant No.

12. Sponsoring Agency Name and Address	13. Type of Report and Period Covered
Anthrotech, Inc. 503 Xenia Avenue Yellow Springs, OH 45387 (NIOSH) Prime	14. Sponsoring Agency Code

15. Supplementary Notes

16. Abstract

Law enforcement officers (LEO) are at relatively high risk of back pain and other musculoskeletal disorders. The risk is exacerbated by the poor accommodation provided by their vehicles, which are usually modified civilian vehicles. LEO are also involved in vehicle crashes at a higher rate than most other occupations, yet officers report difficulty in wearing a safety belt due to interference with their body-borne equipment. To begin to address these issues, a pilot study was conducted to demonstrate the application of three-dimensional anthropometric techniques to quantifying the influence of body-borne gear on space claim and posture in vehicles. The results demonstrated that three exemplar vehicles accommodated the officers poorly due to interference between the seat or other vehicle features and the body-borne gear. Belt fit was also adversely affected, and vehicle modifications and additions, such as the now-common center-mounted laptop computer, create awkward postures for driving, in-vehicle work, and ingress and egress. A large-scale, population-based study aimed at developing seat and vehicle design guidelines using three-dimensional anthropometric techniques is needed.

17. Key Words	18. Distribution Statement
law enforcement officers, anthropometry, safety, vehicle occupants	Unlimited

19. Security Classification (of this report)	20. Security Classification (of this page)	21. No. of Pages	22. Price
None	None	60	

SI* (MODERN METRIC) CONVERSION FACTORS

APPROXIMATE CONVERSIONS TO SI UNITS

Symbol	When You Know	Multiply By	To Find	Symbol
		LENGTH		
in	inches	25.4	millimeters	mm
ft	feet	0.305	meters	m
yd	yards	0.914	meters	m
mi	miles	1.61	kilometers	km
		AREA		
in^2	square inches	645.2	square millimeters	mm^2
ft^2	square feet	0.093	square meters	m^2
yd^2	square yard	0.836	square meters	m^2
ac	acres	0.405	hectares	ha
mi^2	square miles	2.59	square kilometers	km^2
		VOLUME		
fl oz	fluid ounces	29.57	milliliters	mL
gal	gallons	3.785	liters	L
ft^3	cubic feet	0.028	cubic meters	m^3
yd^3	cubic yards	0.765	cubic meters	m^3
	NOTE: volumes greater than 1000 L shall be shown in m^3			
		MASS		
oz	ounces	28.35	grams	g
lb	pounds	0.454	kilograms	kg
T	short tons (2000 lb)	0.907	megagrams (or "metric ton")	Mg (or "t")
		TEMPERATURE (exact degrees)		
°F	Fahrenheit	5 (F-32)/9 or (F-32)/1.8	Celsius	°C
		ILLUMINATION		
fc	foot-candles	10.76	lux	lx
fl	foot-Lamberts	3.426	$candela/m^2$	cd/m^2
		FORCE and PRESSURE or STRESS		
lbf	poundforce	4.45	newtons	N
lbf/in^2	poundforce per square inch	6.89	kilopascals	kPa

APPROXIMATE CONVERSIONS FROM SI UNITS

Symbol	When You Know	Multiply By	To Find	Symbol
		LENGTH		
mm	millimeters	0.039	inches	in
m	meters	3.28	feet	ft
m	meters	1.09	yards	yd
km	kilometers	0.621	miles	mi
		AREA		
mm^2	square millimeters	0.0016	square inches	in^2
m^2	square meters	10.764	square feet	ft^2
m^2	square meters	1.195	square yards	yd^2
ha	hectares	2.47	acres	ac
km^2	square kilometers	0.386	square miles	mi^2
		VOLUME		
mL	milliliters	0.034	fluid ounces	fl oz
L	liters	0.264	gallons	gal
m^3	cubic meters	35.314	cubic feet	ft^3
m^3	cubic meters	1.307	cubic yards	yd^3
		MASS		
g	grams	0.035	ounces	oz
kg	kilograms	2.202	pounds	lb
Mg (or "t")	megagrams (or "metric ton")	1.103	short tons (2000 lb)	T
		TEMPERATURE (exact degrees)		
°C	Celsius	1.8C+32	Fahrenheit	°F
		ILLUMINATION		
lx	lux	0.0929	foot-candles	fc
cd/m^2	$candela/m^2$	0.2919	foot-Lamberts	fl
		FORCE and PRESSURE or STRESS		
N	newtons	0.225	poundforce	lbf
kPa	kilopascals	0.145	poundforce per square inch	lbf/in^2

*SI is the symbol for the International System of Units. Appropriate rounding should be made to comply with Section 4 of ASTM E380.
(Revised March 2003)

Acknowledgements

This research was funded by the U.S. National Institute for Occupational Safety and Health through a contract with Anthrotech, Inc. We thank our volunteers from the University of Michigan Police Department. Many people at UMTRI contributed to the success of this project, including Laura Malik, Kyle Boyle, Emily Lancaster, Lindsay Podsiadlik, Devon Kishore.

Contents

List of Figures

List of Tables

1 Abstract

Law enforcement officers (LEO) are at relatively high risk of back pain and other musculoskeletal disorders. The risk is exacerbated by the poor accommodation provided by their vehicles, which are usually modified civilian vehicles. LEO are also involved in vehicle crashes at a higher rate than most other occupations, yet officers report difficulty in wearing a safety belt due to interference with their body-borne equipment. To begin to address these issues, a pilot study was conducted to demonstrate the application of three-dimensional anthropometric techniques to quantifying the influence of body-borne gear on space claim and posture in vehicles. The results demonstrated that three exemplar vehicles accommodated the officers poorly due to interference between the seat or other vehicle features and the body-borne gear. Belt fit was also adversely affected, and vehicle modifications and additions, such as the now-common center-mounted laptop computer, create awkward postures for driving, in-vehicle work, and ingress and egress. A large-scale, population-based study aimed at developing seat and vehicle design guidelines using three-dimensional anthropometric techniques is needed.

2 Introduction

Law enforcement officers (LEO) make extensive use of vehicles to perform their jobs, often spending large portions of a shift behind the wheel. Few LEO vehicles are purpose-built; the vast majority are modified civilian vehicles. Data from the field indicate that LEOs suffer from relatively high levels of musculoskeletal injury that may be due in part to a mismatch between their vehicles and the physical requirements of accommodating officers and their gear. Moreover, LEOs are exposed to elevated crash injury risk, which may be exacerbated by a compromise in the performance of the occupant restraint systems due to body-borne armor and body-borne equipment (Clark and Zak 1999, Maguire et al., 2002; Oron-Gilad et al., 2005; Tiesman et al., 2010). Fatalities among LEOs in the U.S. are nearly as likely to be due to traffic incidents as homicide, and 58% of LEOs traffic fatalities occur to vehicle drivers (Tiesman et al. 2010).

One barrier to improvements in vehicle accommodation and restraint system performance for LEOs is a lack of detailed anthropometric data for this population. Anthrotech, Inc. is leading a pilot program funded by the National Institute for Occupational Safety and Health (NIOSH) to develop methods for conducting a nationwide survey of LEOs anthropometry. This report documents a small-scale pilot study to demonstrate the potential of three-dimensional scanning and measurement technology to address critical concerns related to vehicle design.

The research objectives were to (1) quantify the effects of LEOs body armor and body-borne equipment on space claim in automotive driver workstations and (2) quantify the effects of LEOs body armor and body-borne equipment on safety belt routing. Five officers from the University of Michigan Police Department participated. The data were used to illustrate applicable measurement methods and to suggest focal points for a large-scale study of this population.

3 Methods

3.1 Overview

Detailed posture and belt fit data were gathered from five law enforcement officers as they sat in the patrol vehicles that they regularly used and in a mockup of a mid-sized vehicle (Figure 1). The mockup had seat belt anchorages that could be configured to represent a range of belt geometries. The size and shape of each officer was measured with and without police uniform and duty belt using standard anthropometry techniques and a whole-body laser scanner. Officers were video recorded getting in and out of their vehicles and performing work tasks inside the vehicle. Officers were asked to volunteer any observations or experiences regarding the vehicles they have used, the equipment that they carry and the interactions between them.

Figure 1. Officers in vehicle, vehicle mockup and being scanned.

3.2 Officer Participants

Five University of Michigan Police Department (UMPD) officers, including one female officer, participated in data collection at the UMTRI facilities in Ann Arbor Michigan. The study protocol was deemed exempt from the University of Michigan Institutional Review Board (IRB) for Health Behavior and Health Sciences (IRB # HUM00101202). Each officer was briefed on the purposes and methods of the study and written consent was obtained.

3.3 Uniform and Equipment Worn by Officers

Officers were tested in their UMPD Class B uniform. All officers wore a soft ballistic vest under the uniform shirt and a duty belt (Figure 2 and Figure 3). Officers wore their own duty belts and equipment.

Figure 2. UMPD uniform with blue tape on gear to make it more visible during scanning and in photos.

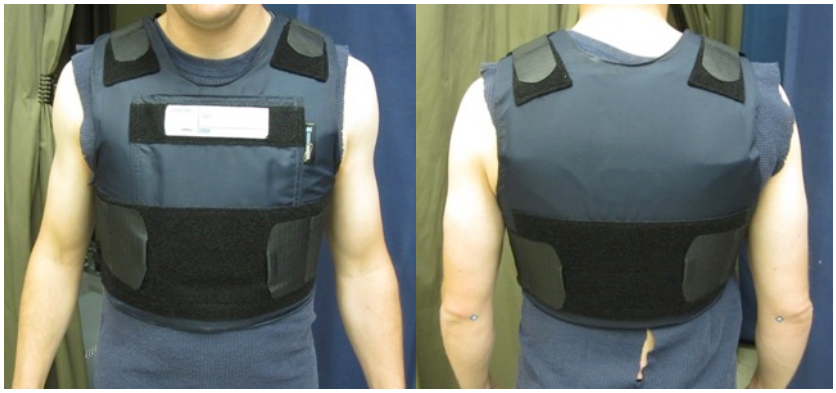

Figure 3. Example of vest worn under clothing (weight approximately 1.6 kg).

The configuration and inventory of equipment on the duty belt varied for each officer in this pilot study. Equipment carried on the duty belt typically included: ammunition magazines, communication radio, flashlight, collapsible baton, ASR (mace), handcuffs, medical kit (tourniquet), gloves, and a side arm weapon (Figure 4-Figure 8). The weight of the duty belt and components is approximately 5.2 kg. Officers configured the equipment along the length of the duty belt based upon individual preference. Belt "keepers" were used to locate individual components along the duty belt and reinforce the attachment of the duty belt to the belt on the pants (Figure 9).

Figure 4. Duty belt worn by one of the officers.

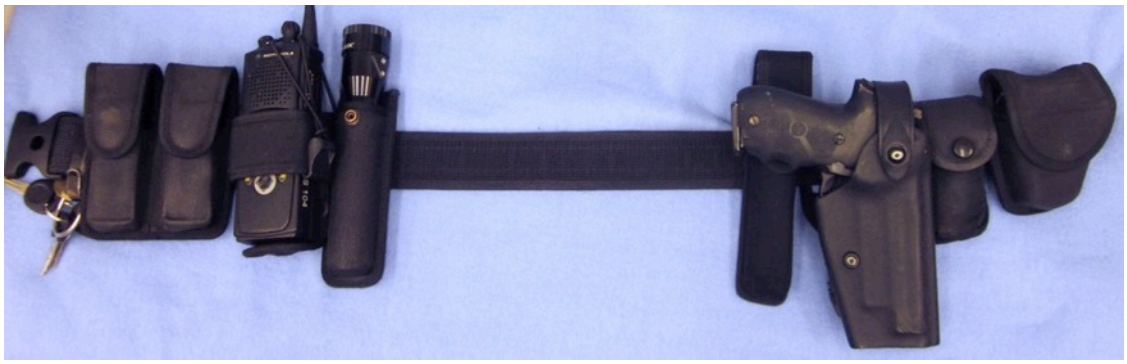

Figure 5. Example officer duty belt laid flat (5.2 kg) which had attached to it from left to right: keys, 2 ammunition magazines, radio, flashlight, collapsible baton, side arm, ASR (mace), and handcuffs.

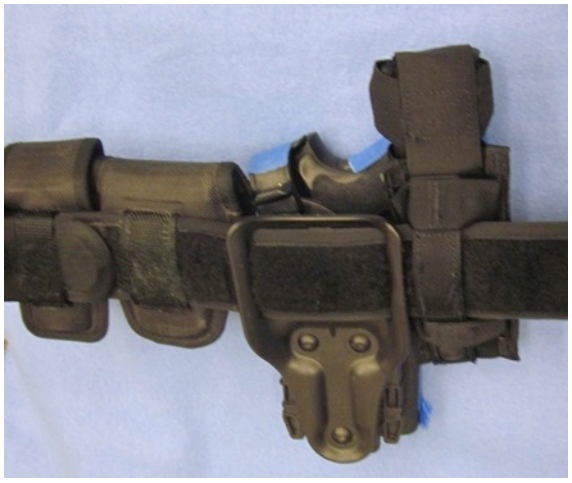

Figure 6. Back Velcro surface of belt.

Figure 7. Tourniquet and utility knife carried in one officer's leg pocket (left) and gloves carried in seat pocket by two officers.

Figure 8. Velcro coated belt worn by officer (left) to which the duty belt is attached (right).

Figure 9. Belt "keepers" (left) that are wrapped around the uniform belt and duty belt (middle) to keep the duty belt from shifting.

3.4 Patrol Vehicles

The vehicle fleet of the UMPD includes three vehicle models: the Ford Taurus, Ford Explorer, and the Chevy Tahoe (Figure 10). The vehicles in this study were from 2011-2015. Vehicles were fitted with audible and visual warning systems (sirens, flashing colored lights), emergency response equipment, two-way radio systems, equipment consoles, suspect transport enclosure (barrier between the 1st and 2nd rows), firearm locker, mobile data terminal, tracking devices (radar), and video cameras (Figure 11-Figure 16).

Figure 10. Examples of a Ford Taurus (above) and Chevy Tahoe (below) from the UMPD fleet.

Figure 11. Interior of the Taurus (left) and Tahoe (right).

Figure 12. Taurus interior.

Figure 13. Tahoe dash.

Figure 14. Center console components and mount for mobile data terminal.

Figure 15. Center console components, which include controls for 2-way radio communication, visual and audible warning systems.

Figure 16. Rifle and charger for voice control for video.

The interior dimensions of both vehicles were measured using a FARO Arm, a three-dimensional coordinate-measurement machine (Figure 17-Figure 18). Some of the surface contour data recorded with the Faro Arm is plotted in Figure 19. The interior surfaces were also recorded with two types of hand-held scanners: a 3DSystems Sense IR scanner and an Artec Eva structure light scanner (Figure 20). H-point measurements were made in each vehicle, using the SAE J826 manikin. The locations of the H-points were recorded with respect to seat surface geometry. All information was referenced relative to reference points on the vehicle frame so that the data could be aligned to the data collected in each officer's vehicle.

Figure 17. Set up for digitizing the Taurus (left), digitizing the H-point location on the J826 H-point machine in the vehicle (right), as well as detailed measurements of vehicle geometry and package layout.

Figure 18. Documenting vehicle interior with hand-held scanners: 3DSystems Sense (left) and Artec Eva (right).

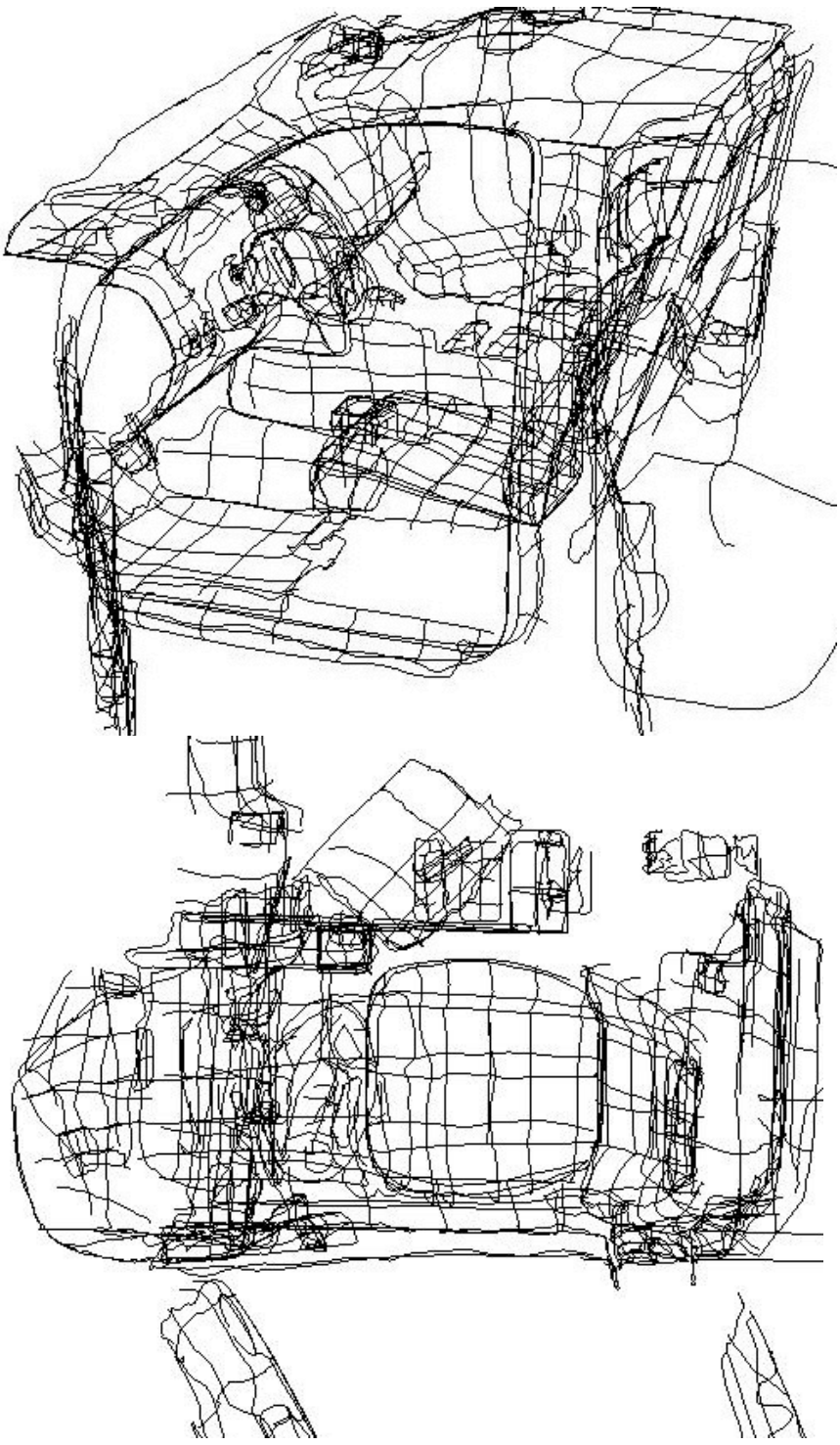

Figure 19. Example of Tahoe stream data.

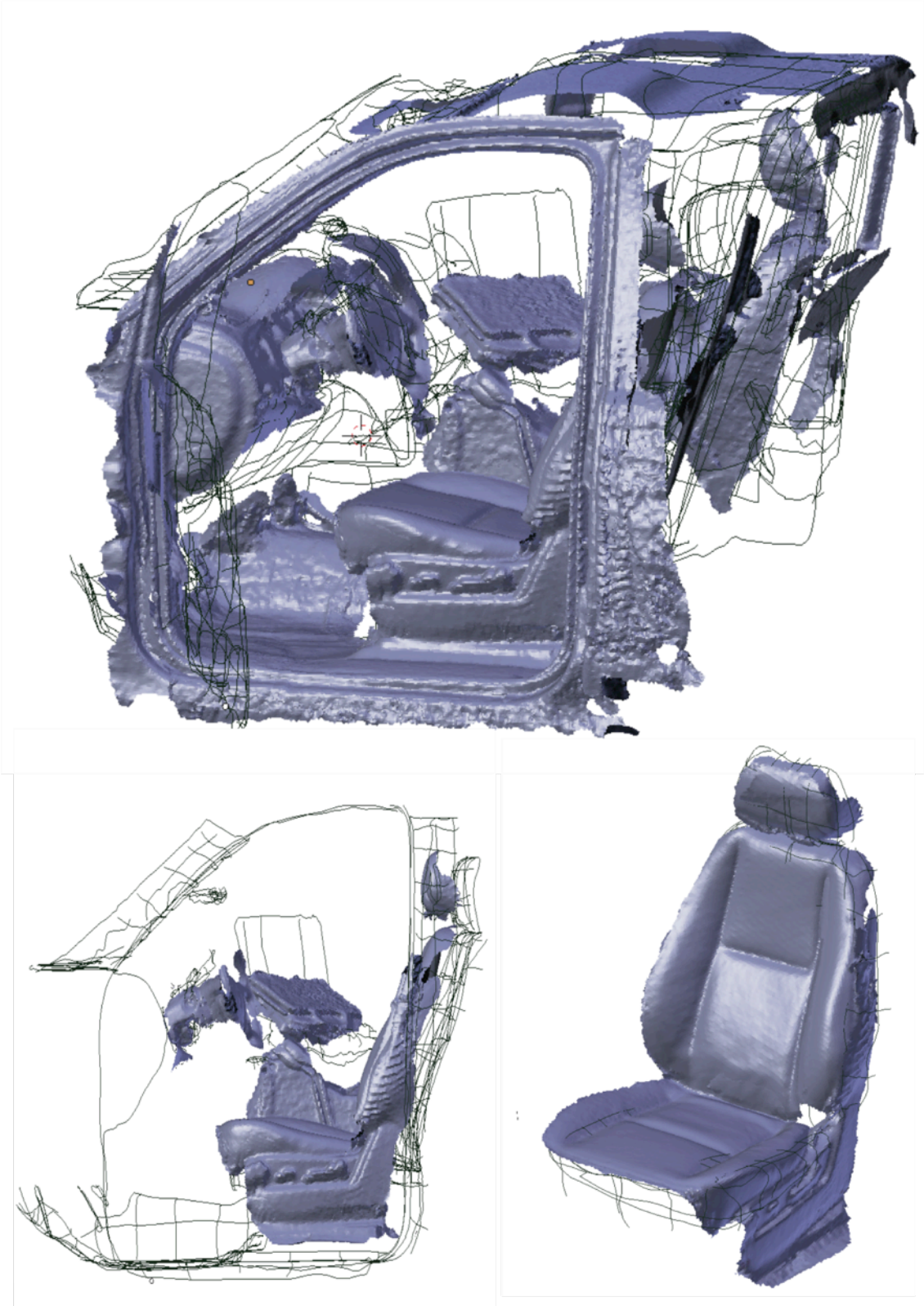

Figure 20. Tahoe stream data superimposed with surface data acquired from 3DSystems Sense.

3.5 Driver Mockup

A driver workstation mockup used in previous studies was modified for use in the current testing. Figure 21 shows the vehicle mockup used for testing. The driver mockup was equipped with a six-way power seat with a power recline adjuster, and a large range of vertical adjustment. The relationships between the seat, steering wheel, and pedals were adjust to represent a wide range of different vehicle packages. The seat was mounted on a motorized platform that could be moved fore-aft so that all subjects were able to select a comfortable seat position without being censored by the available seat track adjustment range. The driver mockup was equipped with a three-point seatbelt with a sliding latch plate. The retractor and D-ring were mounted to a fixture allowing the D-ring location to be adjusted over a wide range. With the D-ring at its typical position, the lower anchorages were adjusted to present the flattest and steepest belt angles permitted under FMVSS 213 (30 and 75 degrees) (Figure 22 and Figure 23).

The test conditions were among those used in several previous UMTRI studies and are designed to span a large percentage of passenger car, light truck, minivan, and SUV packages. Testing was conducted in a range of conditions distinguished by values of steering wheel fore-aft position (SAE L6 or L11), steering wheel height above the heel surface (SAE H17), and seat height (SAE H30). The pedal plane angle was also changed according to SAE J1516 for each seat height. The steering wheel angle was varied at each seat height. Points captured with the FARO arm are listed in Table 2.

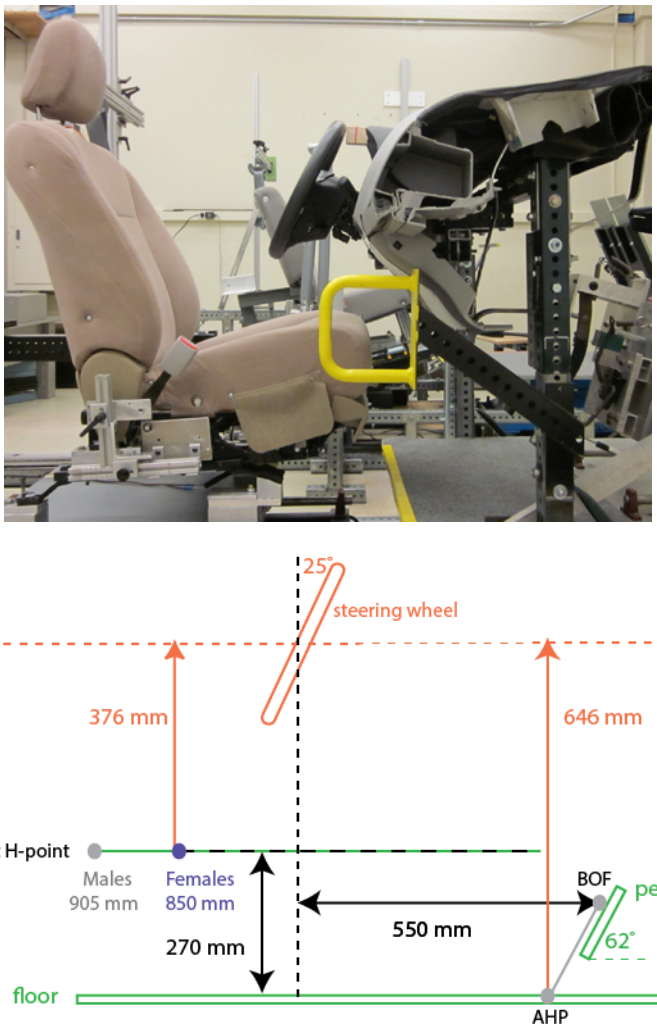

Figure 21. Illustration of one of the package conditions in driver mockup (mm and deg). Steering wheel dimensions reference accelerator heel point. Not to scale.

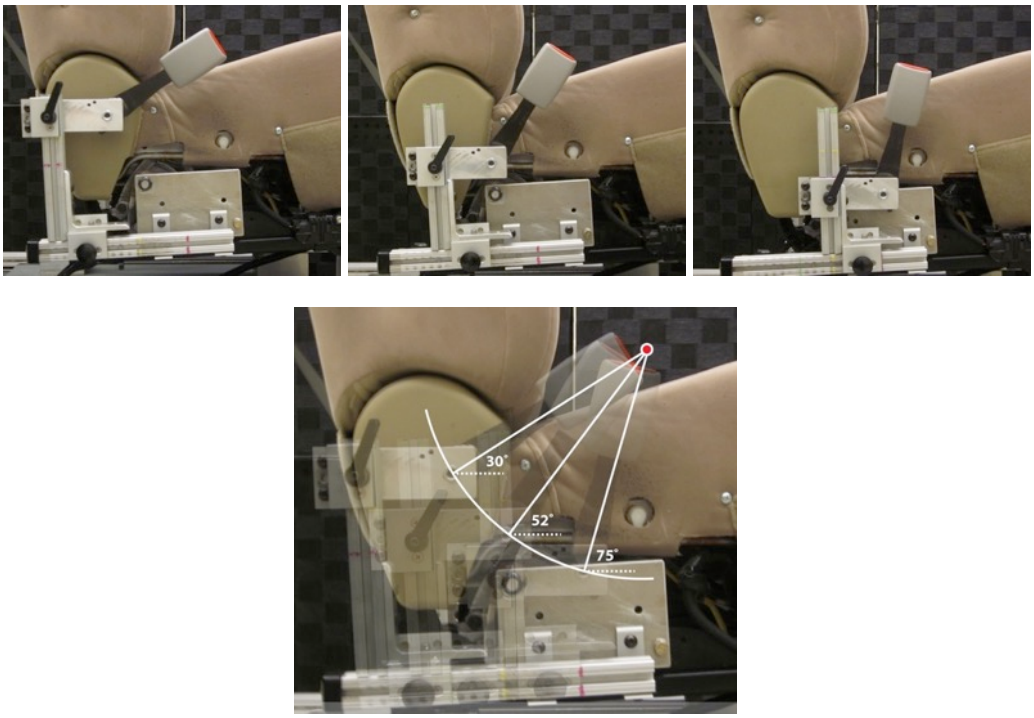

Figure 22. Lap belt buckle anchorage locations for belt fit conditions at 30, 52, and 75 degrees to horizontal.

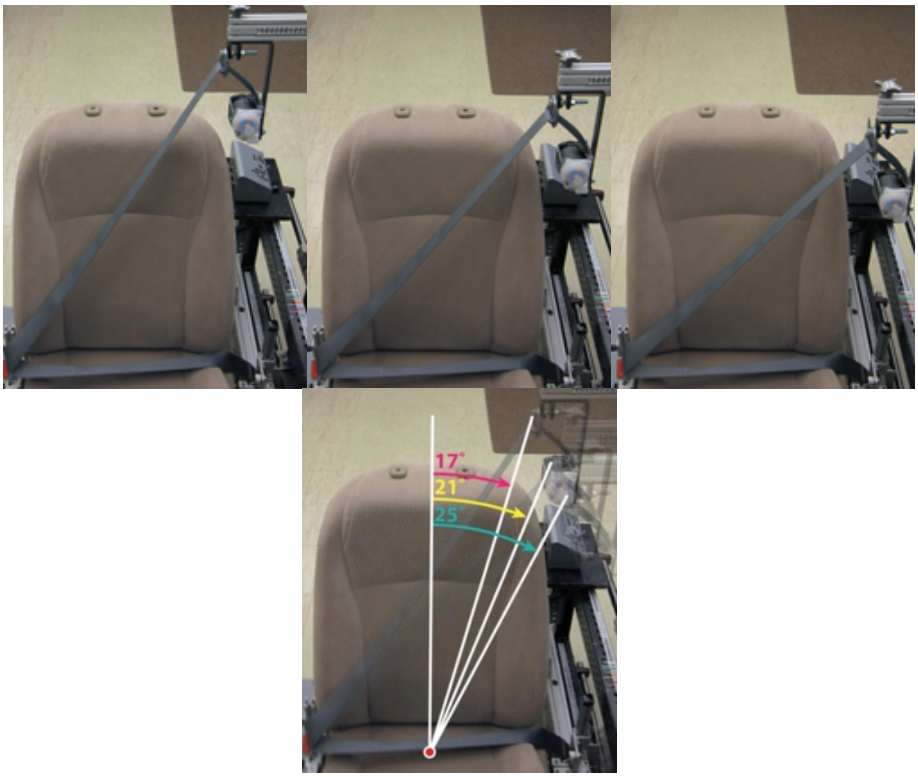

Figure 23. Illustration of shoulder belt conditions with (left to right) YZ angles of 17, 21, and 25 degrees.

3.6 Protocol

The study protocol was deemed exempt by the University of Michigan Institutional Review Board (IRB) for Health Behavior and Health Sciences (IRB # HUM00101202). Each officer was briefed on the purposes and methods of the study and written consent was obtained. All participants were University of Michigan Police Department (UMPD) officers and licensed drivers.

3.7 Testing Protocol in Vehicle

Officers arrived at testing in the vehicle they preferred to drive while on duty. All officers chose to report in Chevy Tahoes, ranging in model years 2011-2015. The driver's normal sitting posture, position, and belt fit were recorded, and the locations of the vehicle components as they were set upon arrival (Figure 24).

Figure 24. Digitizing officer and seat belt.

Table 1 lists the body landmarks and vehicle points that were recorded.

Table 1: Body Landmark and Vehicle Point List

Body Landmark:	**Vehicle:**
C7 (Cervicale)	Accelerator Pedal (6 Points)
Back Of Head Max Rearward	Brake (4 Points)
Top Of Head Max Height	Center Console (8 Points)
Tragion Lt	Floor at Heel Location
Ectoorbitale Lt	Ground Outside Vehicle
Infraorbitale at Pupil Center Lt	Rocker Panel (2 Points)
Glabella	Door opening at B-Pillar (2 Points)
Suprasternale	Instrumental Panel Center
Substernale	Steering Wheel (3 Points)
Medial Clavicle Lt	Shifter
Lateral Clavicle Lt	Head Restraint Center
Acromion Lt (Anterior)	Seat Bight Center
Lateral Humeral Epicondyle Lt (elbow)	Seat Waterfall Center
Ulnar Styloid Process, Lateral Lt (wrist)	Stream of Seat Center and Ceiling
ASIS Lt and Rt	
Suprapatella Lt and Rt	
Infrapatella Lt and Rt	
Lateral Femoral Epicondyle Lt (knee)	**Vehicle Restraint System:**
Bottom edge of sole, longest shoe pt Lt	Outboard Lower Anchor
Ball of Foot Lateral Lt	Inboard Lower Anchor
Lateral Malleolus Lt (ankle)	Buckle
Heel Lt and Rt (Bottom edge of sole at midline)	D-ring (3 Points)
Medial Femoral Epicondyle Rt	TB* location on Clavicle Outboard
Ball of Foot Medial Rt	TB location on Clavicle Outboard
Medial Malleolus Rt	TB location on Midline of Body Top
	TB location on Midline of Body Bottom
LEO Equipment:	TB at Suprasternale Height
Reference stickers on each Duty Belt Item	LB Top at ASIS Lateral Location Lt and Rt
	LB Bottom at ASIS Lateral Location Lt and Rt
Stream Equipment: Duty Belt	LB Top and Bottom at Body Midline
Letters Q & P on Laptop	
Front Corners of Laptop	
Radio Remote Control	Stream Belts: Torso and Lap Belt
Radio Control	
Rifle Release Button	
Video Control	

*TB = torso belt and LB = lap belt

Officers arrived and were video recorded getting in and out of their vehicles, and performing work tasks while seated in the vehicle (Figure 25).

Figure 25. Video recorded tasks.

3.8 Testing Protocol in Driver Mockup

While seated in the driving mockup, the participant was trained in the operation of each seat adjuster and demonstrated use of the components for the investigator. The initial positions of each participant-adjustable component were set to the same midrange values prior to each trial. The participant entered the mockup and adjusted the seat (fore-aft position, vertical position, cushion angle, backrest angle) to obtain a comfortable driving posture. The participant then donned the safety belt and assumed a normal driving posture.

The investigator used the FARO Arm coordinate digitizer to record the three-dimensional locations of landmarks on the participant's body and body-borne gear, and on the mockup, seat, and belt (Table 2). In addition, a stream of points on approximately 5-mm spacing was recorded along the edges of lap and shoulder portions of the belt between the anchorages and latch plate. These data quantify the length of webbing and its routing with respect to the participant.

The officers were measured in their uniforms first and then changed into test clothing (loose-fitting short-sleeve shirt and pants) (Figure 26- Figure 27). The belt fit test matrix was repeated for the minimally clad condition (Table 3).

Table 2: Landmarks and Reference Points Recorded in Driver Mockup

Body Landmarks:	
C7 (Cervicale)	**Vehicle:**
Back Of Head Max Rearward	Accelerator Pedal
Top Of Head Max Height	Floor
Tragion Lt	Platform
Ectoorbitale Lt	Steering Wheel Center
Infraorbitale at Pupil Center Lt	Seat Cushion References (3 Points)
Glabella	Seat Back References (2 Points)
Suprasternale	Reference stickers on each Duty Belt Item
Substernale	
Medial Clavicle Lt	**Vehicle Restraint System:**
Lateral Clavicle Lt	Outboard Lower Anchor
Acromion Lt (Anterior)	Buckle
Lateral Humeral Epicondyle Lt (elbow)	D-ring
Ulnar Styloid Process, Lateral Lt (wrist)	TB* location on Clavicle Outboard
ASIS Lt and Rt	TB location on Clavicle Outboard
Suprapatella Lt and Rt	TB location on Midline of Body Top
Infrapatella Lt and Rt	TB location on Midline of Body Bottom
Lateral Femoral Epicondyle Lt (knee)	TB at Suprasternale Height
Bottom edge of sole, longest shoe pt Lt	LB Top at ASIS Lateral Location Lt and Rt
Ball of Foot Lateral Lt	LB Bottom at ASIS Lateral Location Lt and Rt
Lateral Malleolus Lt (ankle)	LB Top and Bottom at Body Midline
Heel Lt and Rt (Bottom edge of sole at midline)	Stream Belts: Torso and Lap Belt Length
Medial Femoral Epicondyle Rt	
Ball of Foot Medial Rt	Stream Equipment: Officer Duty Belt
Medial Malleolus Rt	

TB= Torso Belt, LB = Lap Belt

Table 3: Belt Anchorage Conditions.

	Upper Anchorage (D-ring)		Lower Anchorages	
	XZ (Fore-aft)	YZ (In-Out)	Outboard	Inboard (Buckle)
1	26.5˚	21˚	52˚	52˚
2	26.5˚	21˚	**30**˚	**30**˚
3	26.5˚	21˚	**75**˚	**75**˚
4	**31.0**˚	**17**˚	52˚	52˚
5	**24.5**˚	**25**˚	52˚	52˚

Figure 26. Officer in mockup in minimally clad condition (light cotton shirt and pants) and in uniform.

Figure 27. Digitizing skeletal landmarks and seat belt locations

3.9 Anthropometry

Anthropometric data were gathered from each officer to characterize overall body size and shape. Standard anthropometric measures were obtained using manual measurements. Table 4 contains a complete list of measurements. All measurements were obtained minimally clad, except that stature was measured with and without footwear to characterize heel height.

Table 4: Standard Anthropometric Dimensions

Weight	Maximum Hip Breadth
Stature (with shoes)	Buttock-Knee Length
Stature (without shoes)	Buttock-Popliteal Length
Erect Sitting Height	Bi-Acromial Breadth
Eye Height (Sitting)	Shoulder Breadth
Acromial Height (Sitting)	Chest Depth (Scapula)
Knee Height	Chest Depth (Spine)
Tragion to Top of Head	Bi-ASIS Breadth
Head Length	Chest Circumference (Axilla)
Head Breadth	Chest Circumference (Bust
Shoulder-Elbow Length	Point)
Elbow-Hand Length	Waist Circumference
	Hip Circumference (Buttocks)
	Upper Thigh Circumference

The investigator used a FARO Arm coordinate digitizer to record the three-dimensional locations of landmarks on the participant's body (Figure 28).

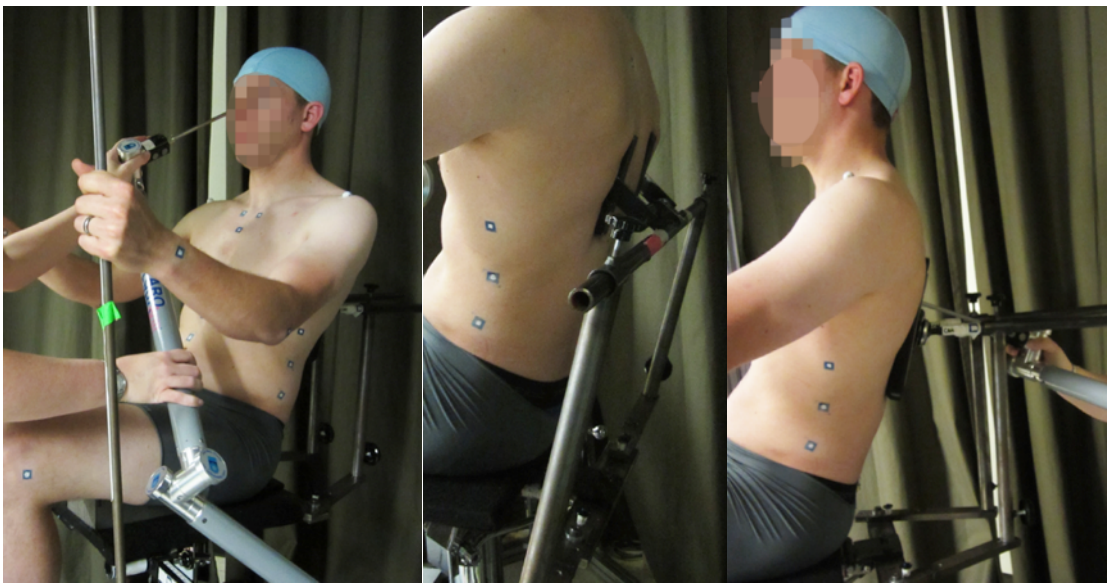

Figure 28. Recording landmark locations with the FARO Arm.

A laboratory hardseat was constructed to enable measurement of the posterior spine and pelvis landmarks such as posterior-superior iliac spines (PSIS) that are inaccessible on the driver mockup (Figure 29). Data on the posterior landmarks are useful in quantifying the participant's skeletal linkage. The hardseat has a 14.5° fixed cushion angle and a 23° fixed seatback angle designed to produce postures similar to those in an automobile seat.

In the patrol vehicle, driver mockup, and hard-seat, the three-dimensional coordinate measuring machine (FARO Arm®, FARO Technology, USA) was used to record the locations of body surface landmarks and seat components. The landmark set and measurement methods were derived from those used in previous studies of adult automotive posture (Reed et al. 1999, Reed et al. 2005).

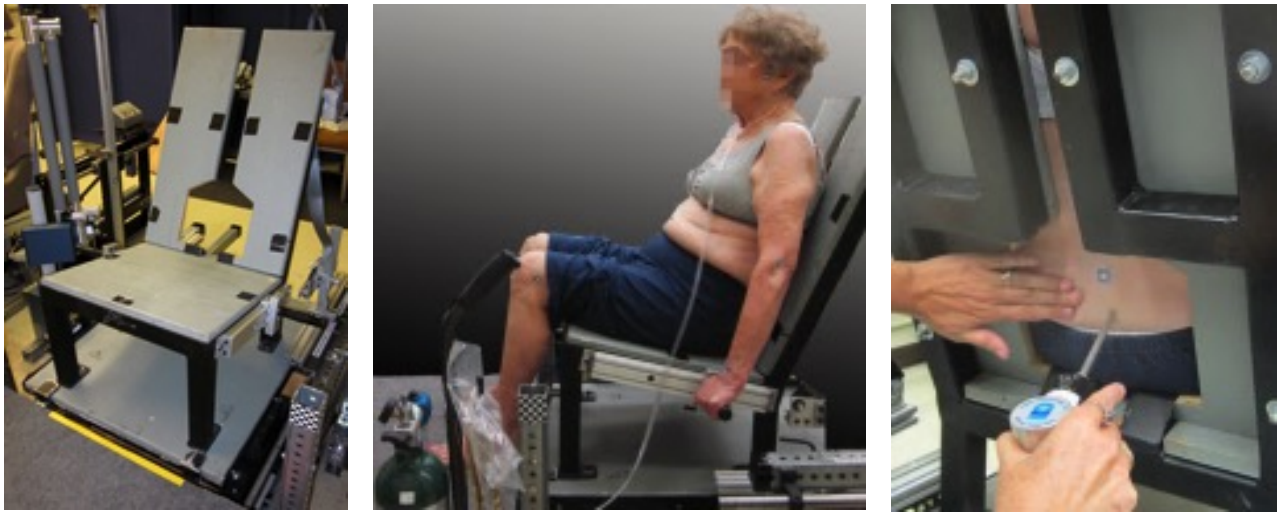

Figure 29. Hardseat and recording a participant's PSIS landmark location using a FARO Arm coordinate digitizer.

3.10 Whole-Body Scanning

Body shape and surface contours were recorded using a Vitronic VITUS XXL full-body laser scanner and Scanworx software by HumanSolutions. The VITUS XXL records hundreds of thousands of data points on the surface of the body in about 12 seconds by sweeping four lasers vertically. The two cameras on each of the four scanning heads pick up the laser light contour projected on the subject and translate the images into accurate three-dimensional data. Figure 30 and Figure 39 show an officer being scanned.

Figure 30. Whole-body laser scanner, with officer in a posture similar to driving. The arms are held away from the body to improve coverage of the torso.

Figure 31 shows the initial scanner setup for the various postures. The scanner also records gray scale images that can be projected onto the 3D surface scan as shown in Figure 32. The locations of landmarks on the participants were recorded via skin targets stamped on the skin using the process shown in Figure 33. The complete list of skin markers is shown in Figure 34. Small hemispheres were taped to the shoulders of the officers to track the location of the acromion landmark. When dressed in the uniform many of the skin stamps were not visible. Instead the right knee of the officer was wrapped with elastic bandages to compress the fabric of the uniform, then in each posture scanned the investigators palpated for the landmarks around the knee and attached targets to the bandage to track their locations. Tape targets were used to track the duty belt.

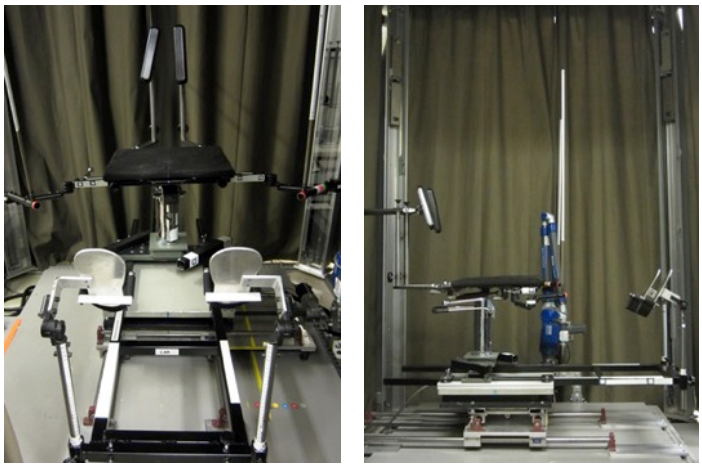

Figure 31. Scanner set up for driver posture, H30=270 mm, back angle = 23˚.

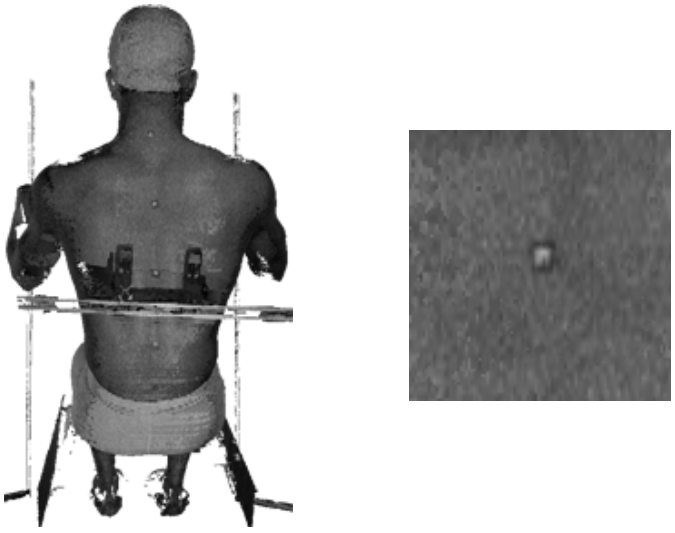

Figure 32. Gray scale image of scan (left) and close-up of stamp used to track landmarks (right).

Figure 33. Marks on a participant used to track body landmarks.

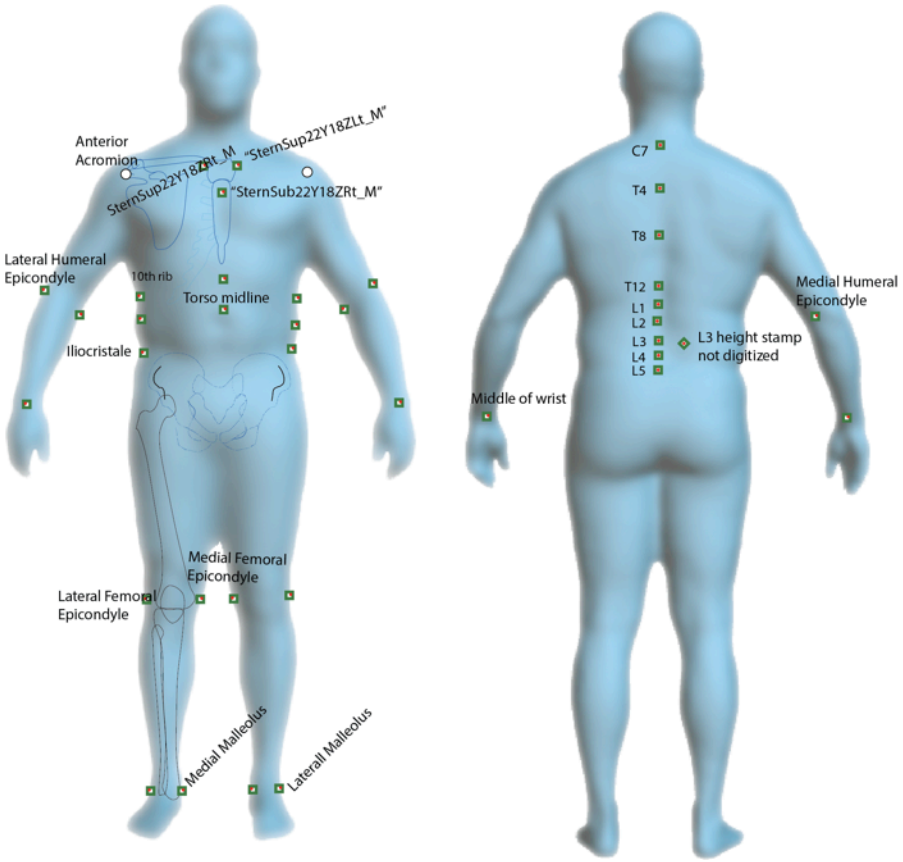

Figure 34. Position of stamped landmarks.

3.11 Scan Postures

All officers were scanned minimally clad and wearing their uniforms. Each participant was scanned in one standing and five seated postures. The postures were chosen from among many considered to capture the range of body shapes expected in automotive seating situations, as well as to characterize the overall body shape in ways that could be compared to other datasets. The supported, seated scans were sagittally symmetric postures (R1, R2, R3, and automotive). R1, R2, and R3 are obtained with a range of recline angles. The automotive posture also includes elevated thighs and extended knees. An unsupported sitting posture was included for reference to other studies and to provide an unobstructed back contour. Table 5 lists the scanning postures, and they are illustrated in Figure 35-Figure 38.

Table 5: Scanning Postures

Posture	Code	Seat Pan	Seat Back	Hips	Lower Limbs	Spine	Shoulders	Hand Scan
Standing T-pose	T1	NA			15 cm	Natural	Abduction 40˚	
Automotive	C1	Wedges (14.5˚)	pads		Driving	Natural	Abduction 90˚	Yes
Recline 1	R1	Wedges (14.5˚)	L2		Knees at 90˚, legs parallel	Min slouch	Handles	Yes
Recline 2	R2		L3			Mid slouch		Yes
Recline 3	R3		L4			Max slouch		Yes
Sitting Lap	L1	0˚	bar	75°	Ankles under the knees, legs parallel	Erect	Handle	

*Handles= Palm at height of Suprasternale, shoulders as if arms were hanging at sides with elbows 45˚ out from body in coronal view and the shoulder-elbow-wrist angle at 120˚

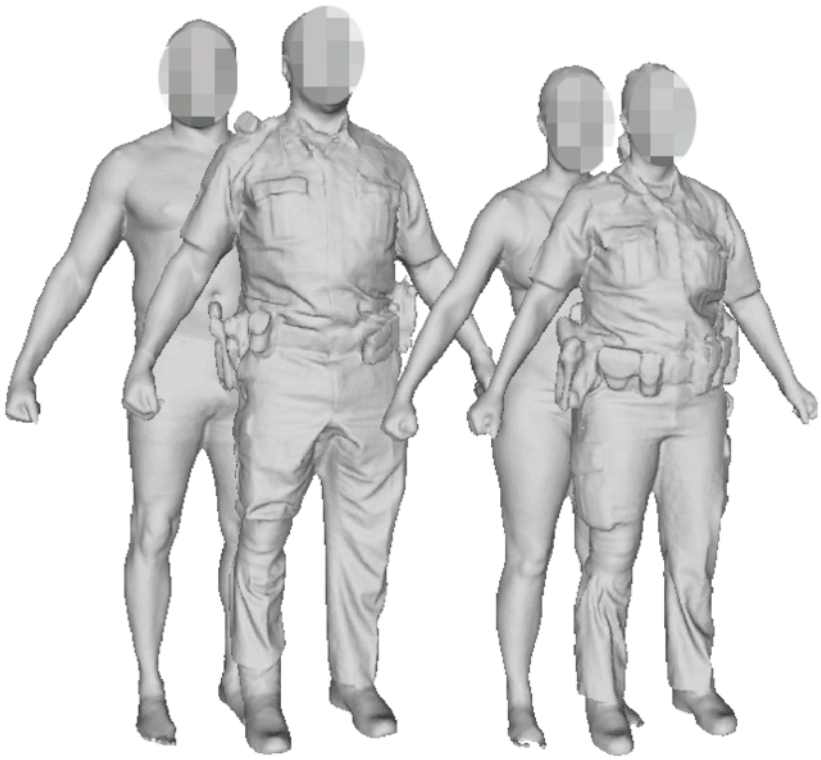

Figure 35. Scan of standing officers (T2).

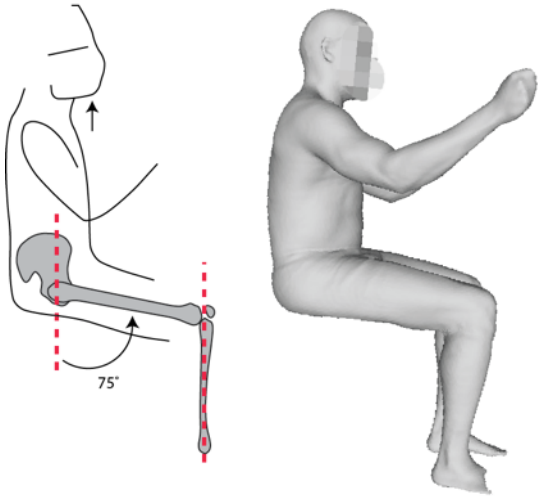

Figure 36. Sitting L1 posture.

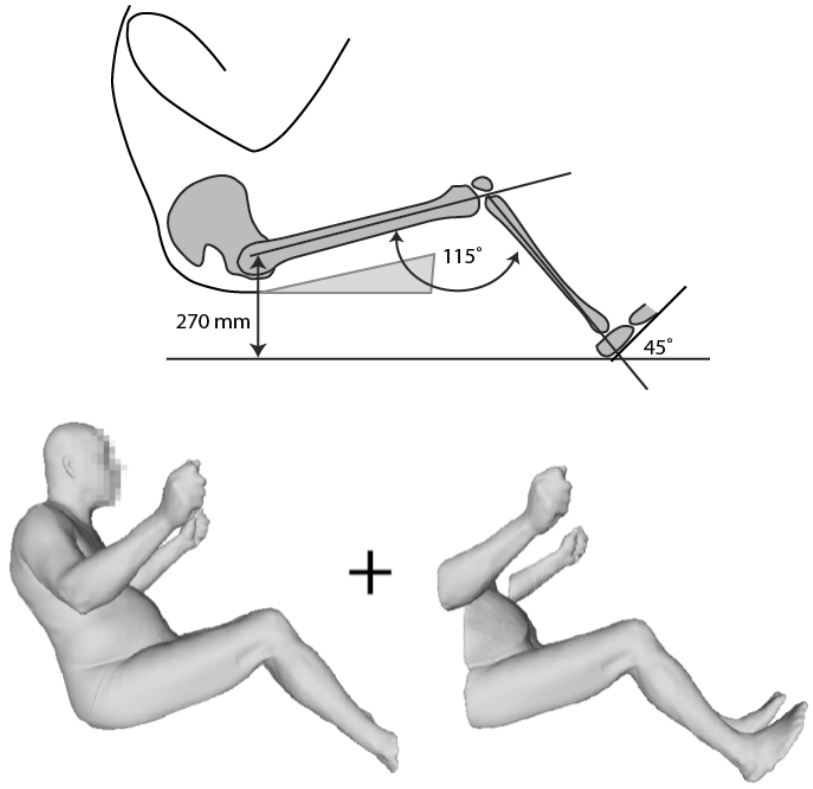

Figure 37. Automotive posture.

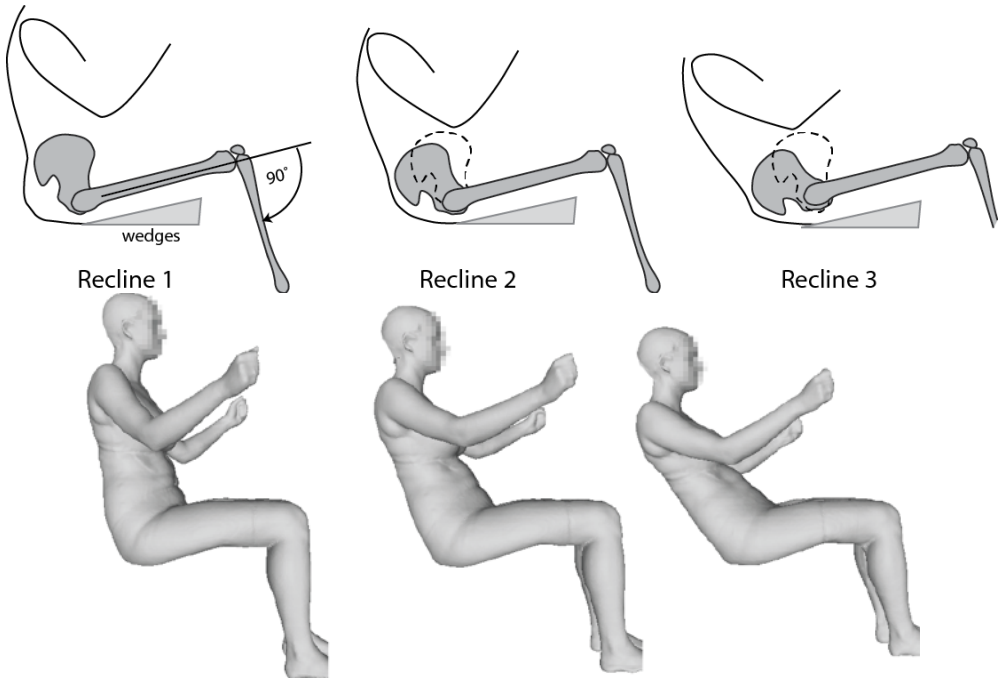

Figure 38. Recline postures 1 through 3 (left to right).

The “recline” scans were a series of three postures in which the subject’s posture went from an erect to very reclined, while maintaining a 90˚ knee angle with legs and feet parallel. To achieve scan coverage of the sides of the torso, the officer’s arms were moved away from the body, but the shoulder position was kept in a relaxed seat position. The investigator set the elbow angle to 120˚, the angle of the arm relative to the midline of the torso in coronal view to 45˚, and the hand height to the Suprasternale Height in the erect posture. The officer was instructed to sit looking forward with relaxed shoulders with the weight of the arms supported by gripping an upright rod and with a relaxed spine in the two more reclined postures (Figure 39).

Figure 39. Officer wearing uniform in reclined postures.

3.12 Measurement of lap and shoulder belt fit

Prior to measure lap belt fit, each participant pelvis location across all the test trials were estimated based on the anatomical and kinematical relationship between body surface landmarks and pelvis bony landmark locations. Reed et al. (2013b) found that flesh margins between actual bone ASIS and digitized body surface ASIS varied with BMI. Reed et al. (2013b, 2014) developed statistical models to predict pelvis bony landmark (ASIS, PSIS, hip joint, and L5/S1) locations in a local pelvic coordinate system. The present study applied the statistical models to predict the participants' pelvis bony landmark locations in the hardseat, and then applied the Park et al. (2015) optimization algorithm to estimate pelvis locations in the rear seat mockup using the digitized body surface landmark data in each test condition.

The lap belt fit was quantified as fore-aft (X) and vertical (Z) distances (unit: mm) from outboard bone ASIS to upper edge location of lap belt in a sagittal plane. The fore-aft lap belt fit is negative forward of ASIS, and the vertical lap belt fit is positive above ASIS (Figure 40a). The shoulder belt fit (Figure 40b) was measured as a lateral (Y) distance (unit: mm) from suprasternale to inboard edge of shoulder belt in a coronal plane. The shoulder belt fit is positive when the inboard edge of shoulder belt lies outboard of the suprasternale.

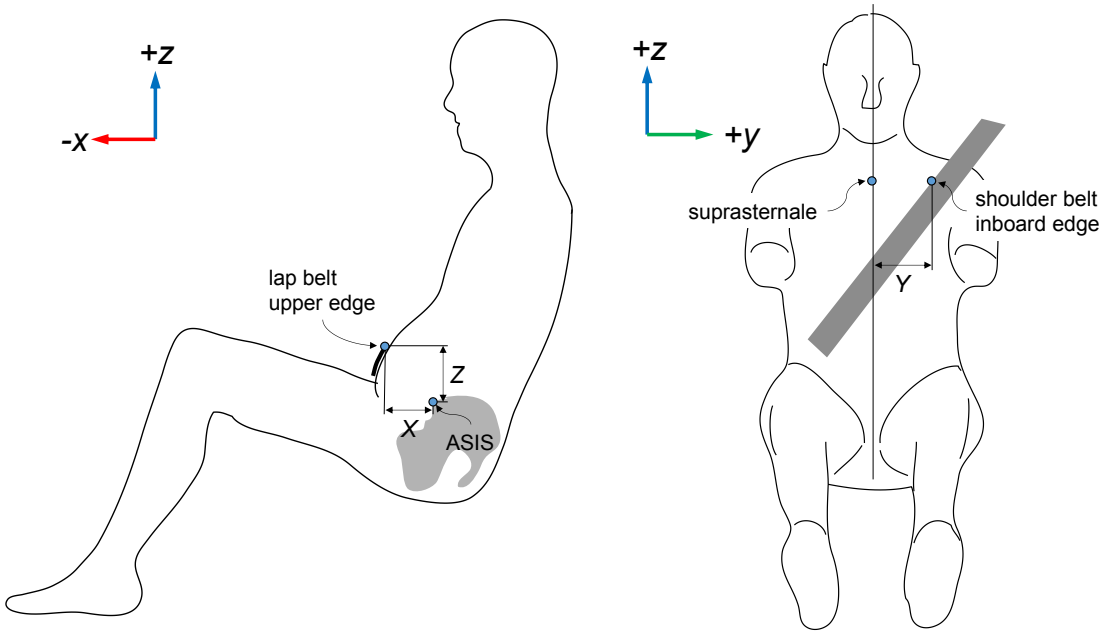

(a) lap belt fit relative to ASIS (b) shoulder belt fit relative to suprasternale

Figure 40. Illustrations of lap and shoulder belt fit.

A fourth-order Bézier curve was fit to the lap and shoulder belt stream points to smooth measurement error and the length of the resulting curves were calculated (Reed et al., 2013b).

4 Results

4.1 Traditional Anthropometry

Five University of Michigan Police Department (UMPD), officers including one female officer, participated in data collection. Table 6 lists the overall body dimensions of the pilot study participants. All but one was overweight (BMI > 25 kg/m^2) but none was obese (BMI > 30 kg/m^2). All were taller than median female stature for civilians (approximately 1630 mm) and one was taller than the 95th-percentile for U.S. male civilians (approximately 1870 mm). Figure 41 shows some of the body shapes captured in the study and Figure 42 shows the same individuals scanned while wearing their gear.

Table 6: Participant Anthropometric Measures.

Subject	Gender	Age (years)	Stature (mm)	Weight (kg)	BMI (kg/m^2)
L2	F	34.3	167.6	72.7	25.9
L1	M	46.8	178.9	91.5	28.6
L3	M	35.5	196.0	107.4	28.0
L4	M	33.7	175.2	75.3	24.5
L5	M	45.8	184.6	100.4	29.6
	Mean	39.2	180.4	89.5	27.3
	SD	6.5	106.6	15.3	29.6

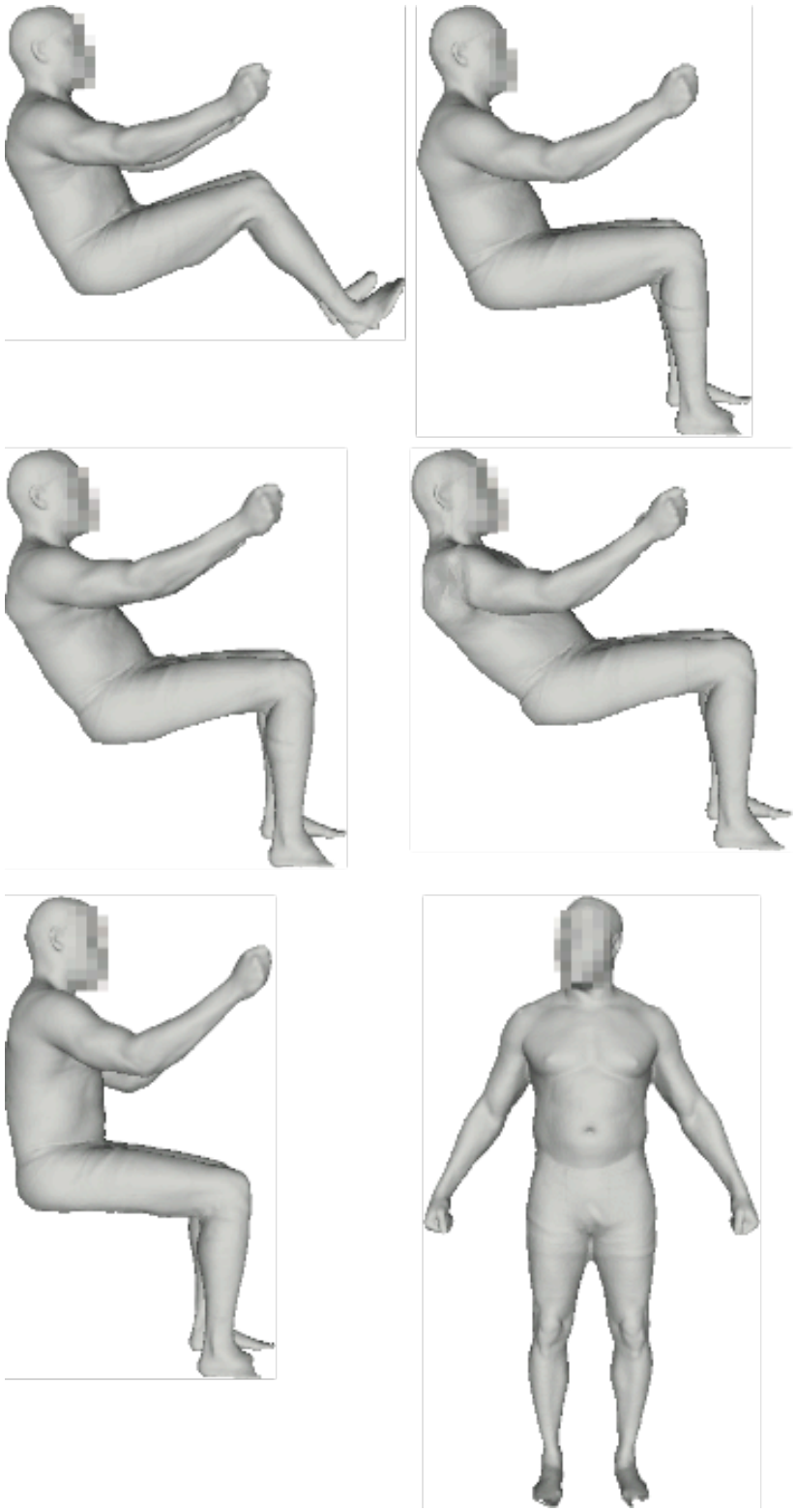

Figure 41. Representative body scans in the standing and seated postures in minimally clad clothing conditions.

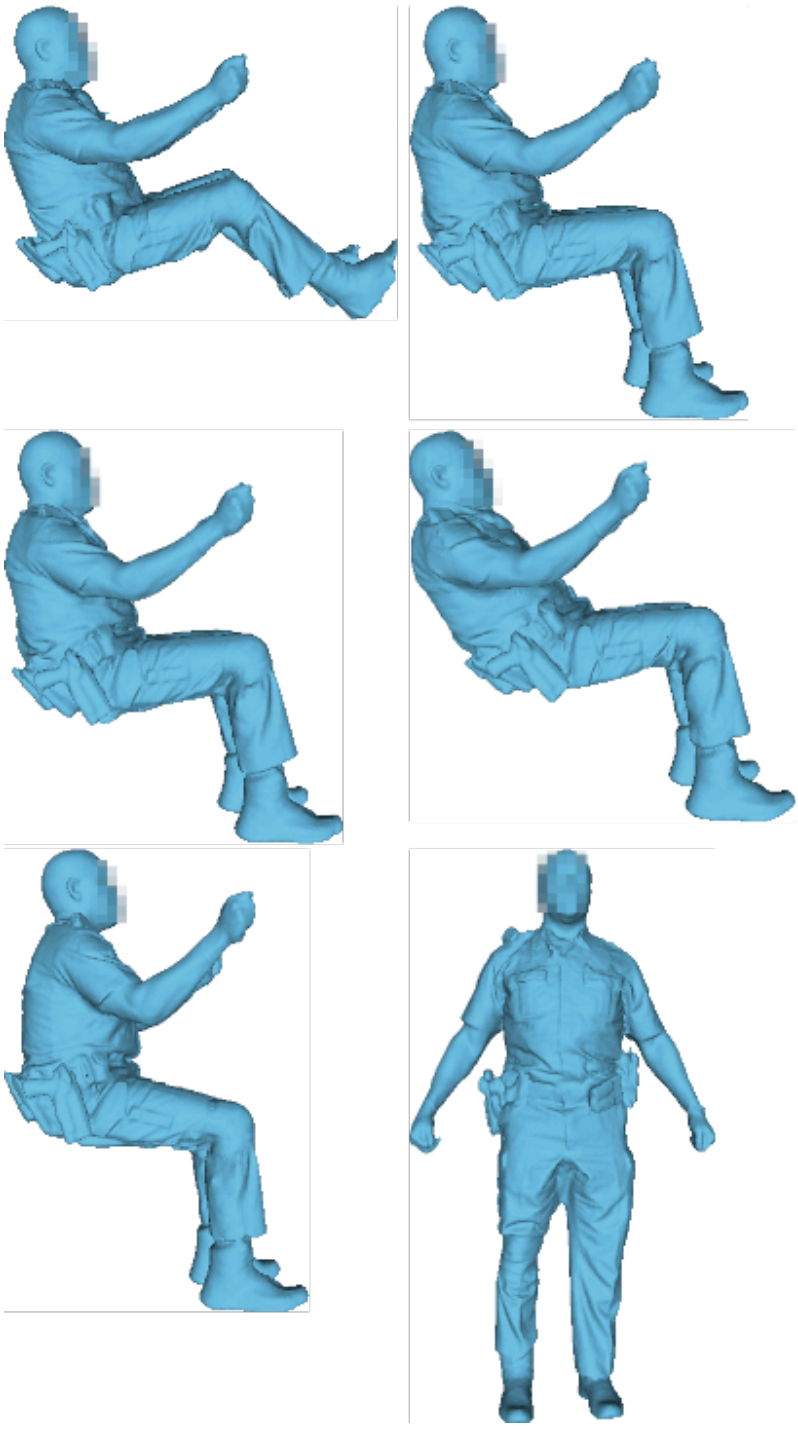

Figure 42. Representative body scans in the standing and seated postures, while donning the LEO uniform and equipment.

4.2 Space Claim Analysis

The effects of the LEO uniform and personal protective equipment on space claim are important for the design of seats and patrol vehicle interiors. Scan data from minimally clad and equipped conditions were overlaid to quantify the increase in space claim resulting from the uniform and body-borne gear. Figure 43 – Figure 45 illustrate the effect of the LEO uniform and duty belt during the unsupported and reclined seated postures. Note the large increase in depth in the posterior hip area due to equipment on the duty belt.

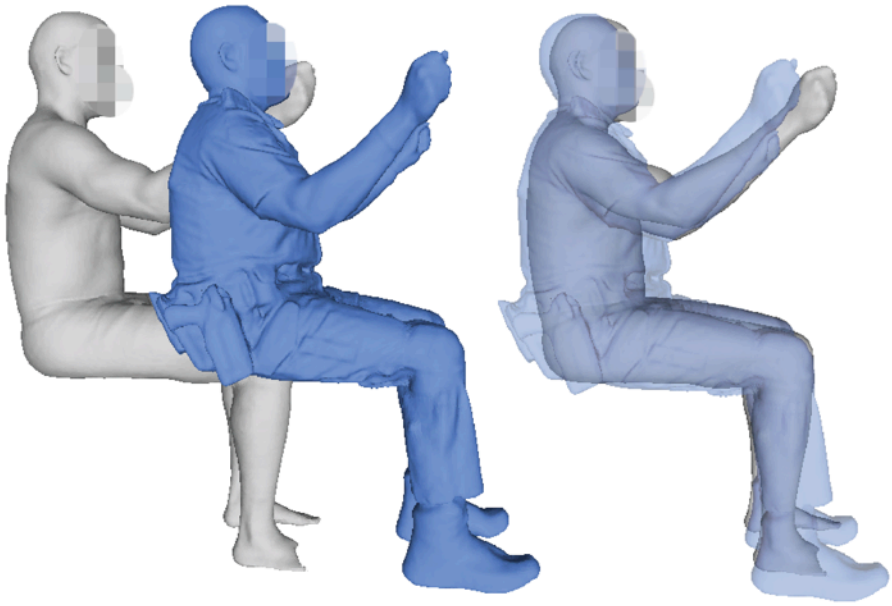

Figure 43. Scan in L1 posture minimally clad and with uniform (side view).

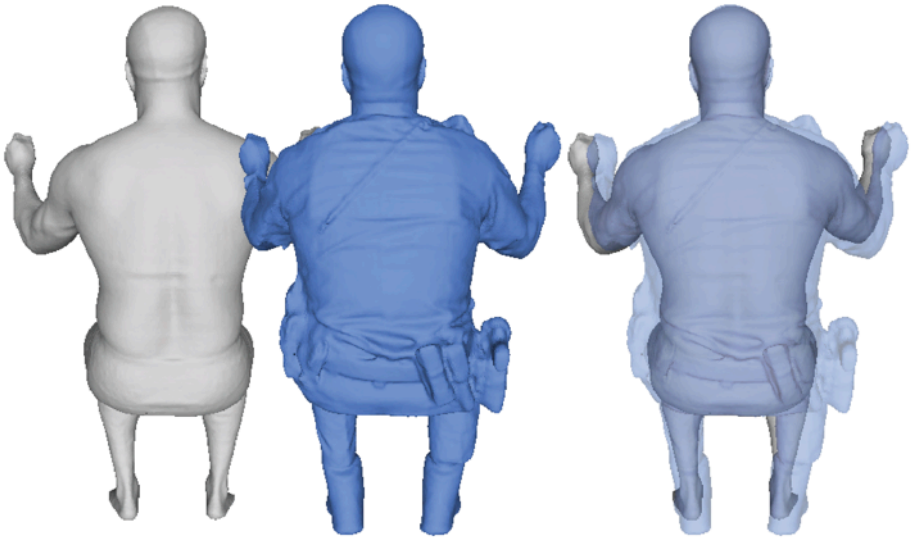

Figure 44. Scan in L1 posture minimally clad and with uniform (rear view). Scans are manually overlaid to demonstrate differences in exterior shape.

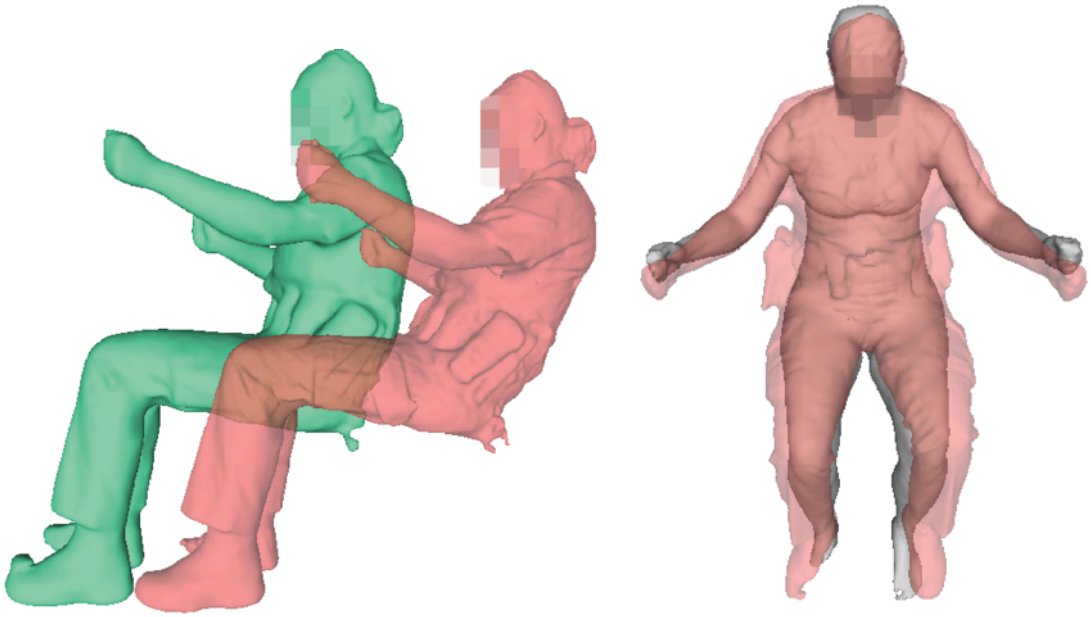

Figure 45. Scan of R1 (green) and R3 (red) in side view (left) and of R3 in uniform (red transparency) over R3 in scanwear. Note the increase in lateral thigh width associated with thigh-borne gear for this female officer.

An examination of the scan data showed that the greatest increase in space requirements for the LEO uniform and equipment is observed at the waist area (Figure 46). A horizontal plane was established at a height associated with the maximal breadth for the equipped condition. Points on the scan within 25 mm of this plane were extracted to characterize the most-lateral, most-forward, and most-rearward dimensions. The same plane was applied to the minimally clad scan data. Figure 47 shows the 2D cross-sections extracted at the waist area to illustrate the increase in space claim resulting from the LEO uniform and equipment.

Figure 46. Side view overlays of scans showing increases in depth.

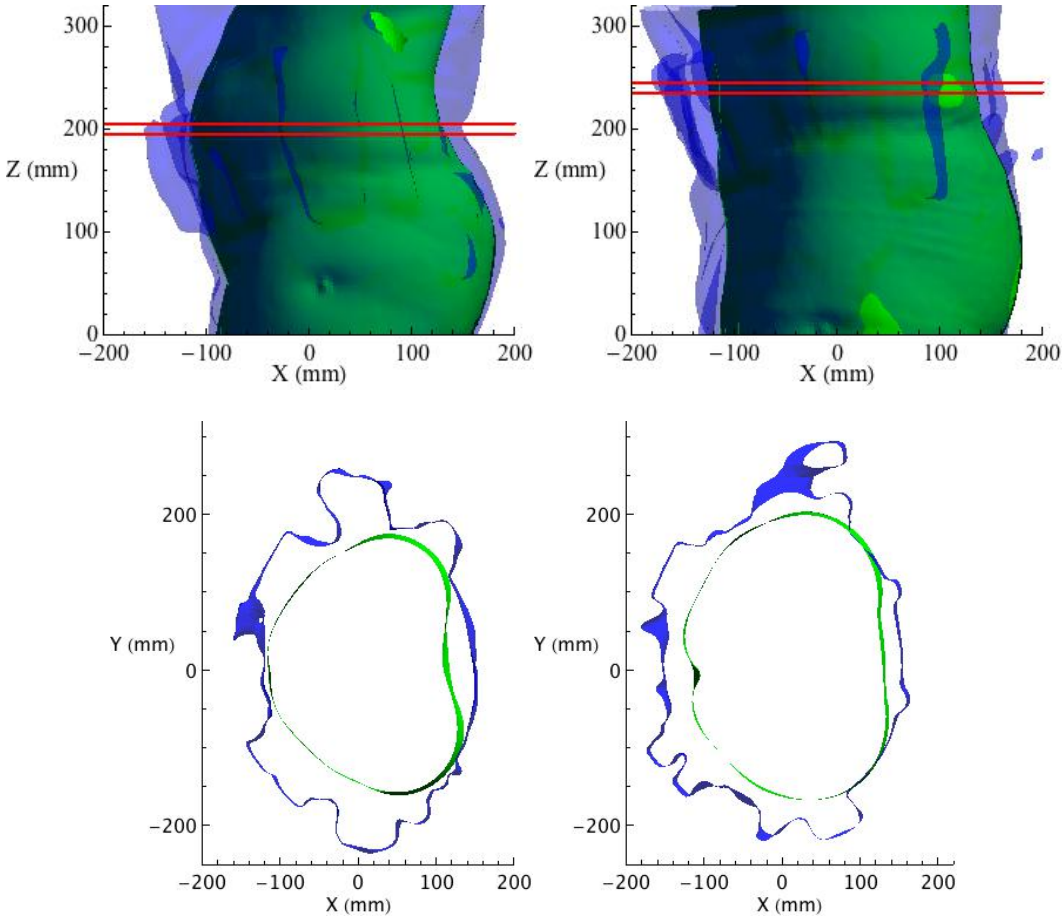

Figure 47. Sections through the waist area (standing)
showing the increased space claim resulting from the duty belt and gear.

Many officers indicated that the duty belt was a primary source of discomfort. Traditional duty belt configurations have equipment located at the back of the duty belt, the equipment will rest against the lower back, creating pressure concentrations and influencing posture. Officers reported that they were able to choose how to configure and distribute equipment along the length of the duty belt and indicated a preference for locating the equipment to the front and side of the belt to minimize the interaction with the vehicle seat. Figure 48 - Figure 49 show some of the variability in duty belt configurations.

Figure 48. Standing space claim analysis for two officers.
The images at the top show the duty belts.

Figure 49. Variability in duty belt configurations.

One study participant was scanned wearing SWAT gear, which includes a helmet and more extensive body armor and gear. Figure 50 shows an overlay of the space claim for this gear, which includes a large amount of posterior equipment that would be expected to interfere with seated posture.

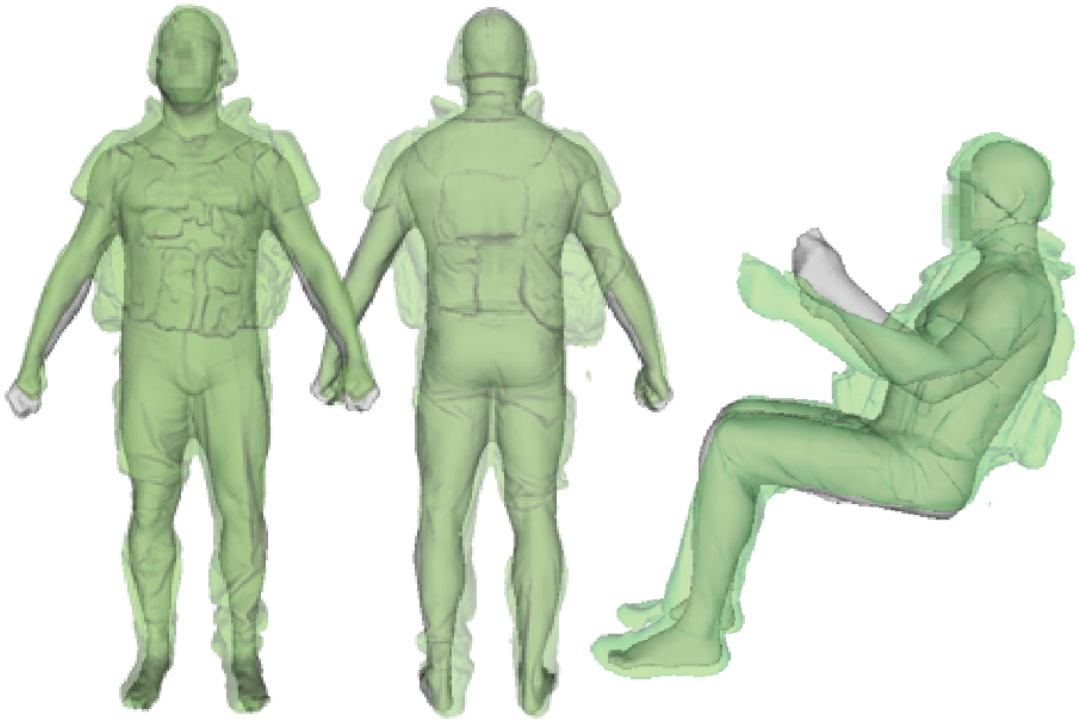

Figure 50. Scan overlay with SWAT team equipment.

4.3 Posture Analysis

The design of these pilot methods was such that the effects of the driver mockup package dimensions (seat height and steering wheel position) could be evaluated in the minimally clad and LEO uniform and equipment conditions. The objective of this method was to quantify the effects of officer body dimensions and the independent experimental variables on a set of measures of posture and position. Various effects of the uniform and duty belt on seated posture were observed. During the mid-belt condition of the driver mock-up, two alternative behaviors were observed in response to the LEO uniform and equipment condition:

- Maintain the seat in same position and shift the pelvis more forward in the seat, or
- Translate the seat rearward and make small adjustments to the hip position to change torso angle.

Figure 51-Figure 55 show overlays of postures and belt routing measured in the middle vehicle mockup and belt condition in light clothing and with full uniform and gear.

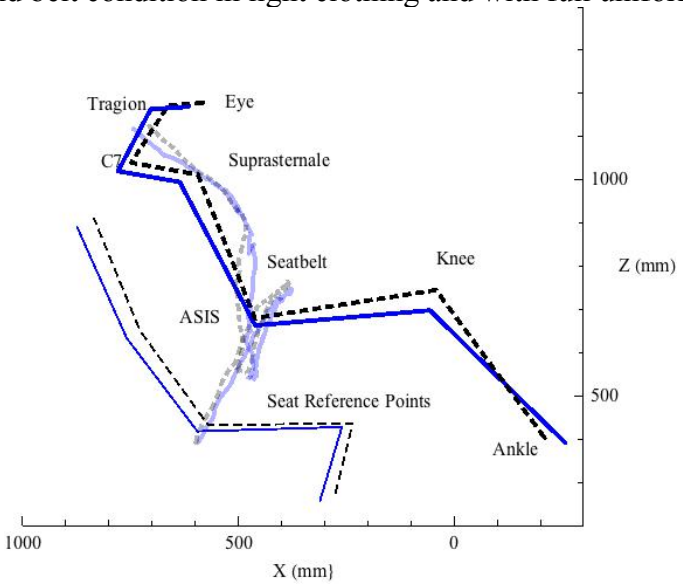

Figure 51. Officer L1 in uniform (solid blue) and light clothing (dashed black). Seat more rearward in uniform, but pelvis in similar position- resulting torso angle more reclined.

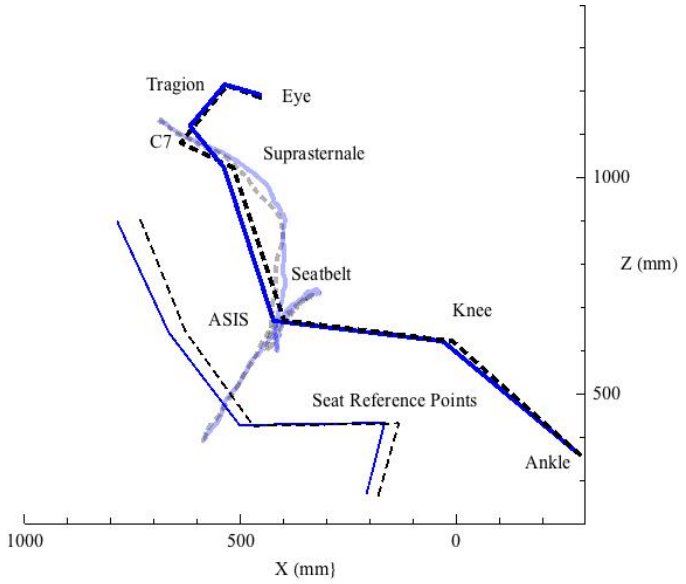

Figure 52. Officer L2 in uniform (solid blue) and light clothing (dashed black). Seat more rearward in uniform, and pelvis shifted rearward slightly – resulting in a more upright torso angle.

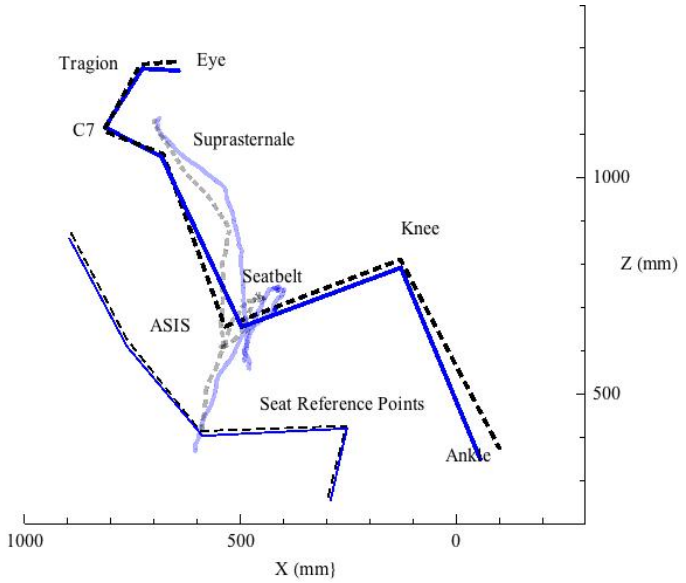

Figure 53. Officer L3 in uniform (solid blue) and light clothing (dashed black). Seat in same position for uniform and light clothing, but the pelvis is more forward in the seat.

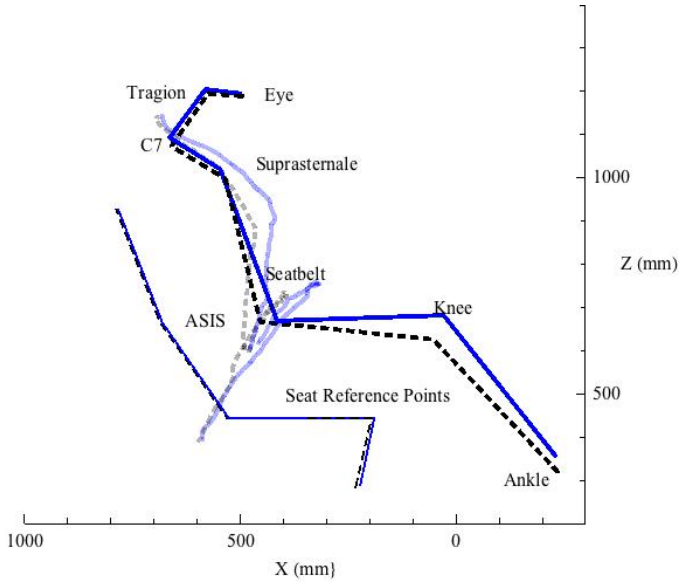

Figure 54. Officer L4 in uniform (solid blue) and light clothing (dashed black). Seat in same position for uniform and light clothing, but the pelvis is more forward in the seat.

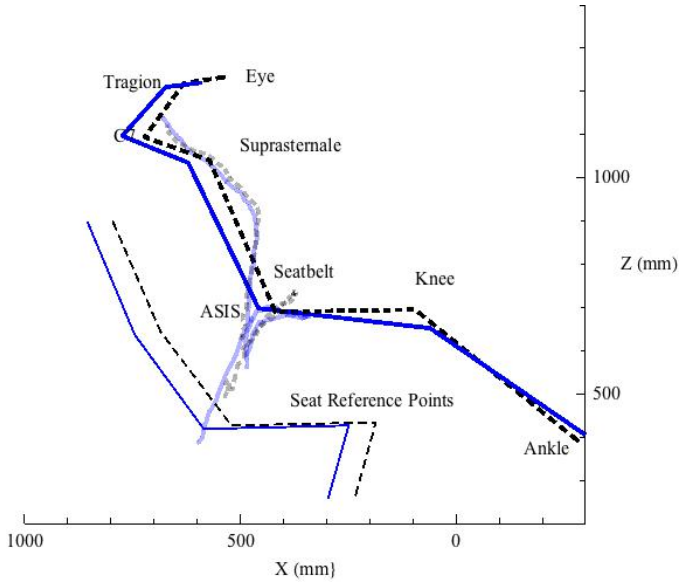

Figure 55. Officer L5 in uniform (solid blue) and light clothing (dashed black). Seat more rearward in uniform, and pelvis shifted rearward – resulting in a slightly more reclined torso angle.

4.4 Safety Belt Routing

Figure 56 shows examples of safety belt routing in the patrol vehicle. Good seat belt designs are easy to don and route the lap portion of the belt low on the pelvis with the shoulder portion of the belt centered on the clavicle. Officers reported difficulty buckling the belt, and the lap portion of the belt was frequently observed to be routed over equipment on the duty belt. This routing adds slack to the belt and may also result in the belt riding up into the abdomen during a crash, rather than performing as intended by directing restraint force onto the pelvis.

Figure 56. In-vehicle lap belt fit -Tahoe (L5).

In the laboratory mockup, interference between the sidearm and buckle was observed for right-handed officers. Figure 57 shows the lap belt location with respect to the anterior-superior iliac spine (ASIS) landmarks on the left and right sides of the pelvis, for male officers in the driver mockup for both light clothing and LEO uniform conditions. Findings indicate that the lap portion of the belt is frequently placed above and well forward of the bony pelvis, due to donning the LEO uniform and equipment. Also, that the lap belt offsets relative to the bony pelvis are asymmetric due to the variability in the duty belt configurations.

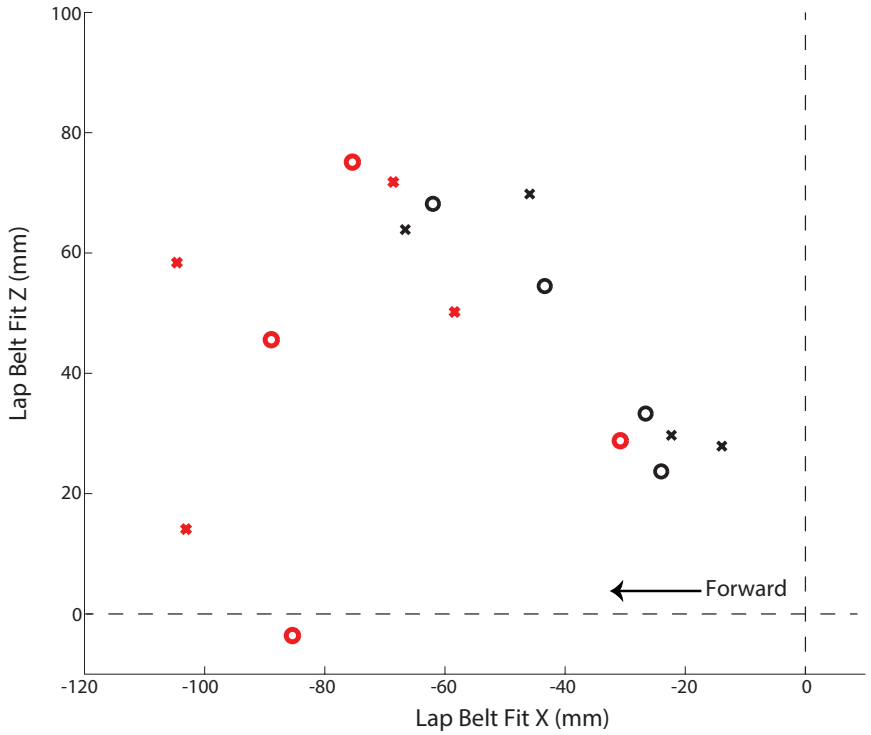

Figure 57. Lap belt location for all trials for light clothing (black) and LEO uniform and equipment (red). The data points are the location of the upper edge of the lap belt at the lateral position of the left (o) and right (x) bone ASIS landmarks relative to the bone ASIS landmark.

Figure 58 and Figure 59 show the poor (high) belt routing that can result. In general, the belt interaction with the equipment was observed to add variability in belt routing that usually resulted in deviations from optimal lap belt positioning.

Figure 58. Restraint in mockup with anchorage set relative to H-point at 30˚, 52˚ and 75˚ which span the range of angles permissible in FMVSS210. Note the routing of the belt.

Figure 59. Lower anchorage angle 30˚ and upper at mid setting.
Note the routing of the belt.

Figure **60** shows the effect of light clothing and LEO uniform and equipment conditions across the shoulder belt matrix trials. To compare LEO uniform and minimally clad fit, the mean ± SD of shoulder belt fit of light clothing was 76.5 ±15.5 mm, and that of LEO uniform and duty belt was 114 ±17.4 mm.

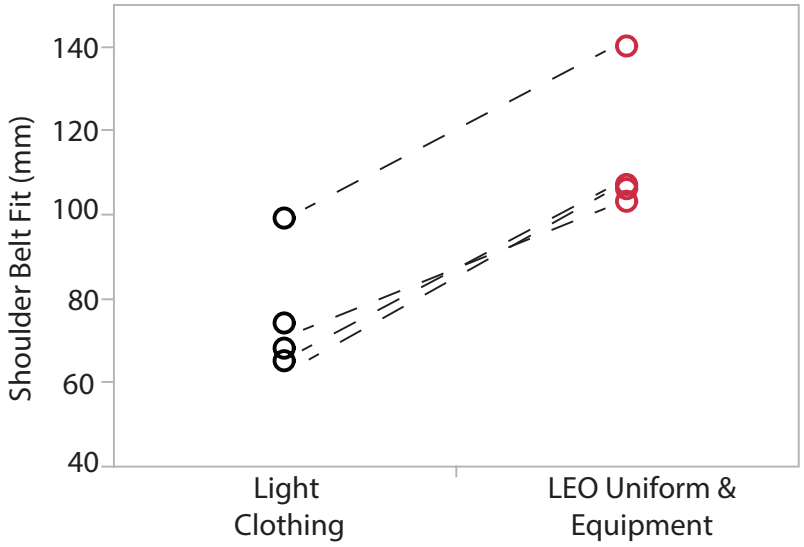

Figure 60. Effect of LEO body-borne equipment on the shoulder belt fit. Light clothing are denoted with black markers and the LEO uniform and equipment are denoted with red.

The laser scan data were combined with belt routing measured in the laboratory seating mockup to examine the shape of the belt paths with respect to the anatomy. Figure **61** and Figure **62** demonstrates that the body borne equipment holds the belt away from the body, resulting in longer belt paths that are farther from the skeletal targets for the belt (pelvis and clavicle). The length of belt webbing between the outboard lower anchorage and the latchplate was calculated from points digitized along the upper/rearward surface of the belt. Because the outer anchorage was attached to the mockup (to simulate an anchorage attached to the vehicle body), the webbing length was strongly affected by driver-selected seat position. Length of the shoulder belt webbing was quantified between the upper anchorage and the outboard lower anchorage. Table 7 highlights the difference in lap and shoulder belt lengths that resulted between the light clothing and LEO uniform conditions during the mid-belt condition.

Table 7: Lap and Shoulder Belt Webbing Length for representative officers.

Lap Belt Length

	LEO Uniform	Test Clothing	Delta
L1	931	850	80.9
L3	863	792	70.8
L4	862	813	48.9
L5	884	771	113.5

Shoulder Belt Length

	LEO Uniform	Test Clothing	Delta
L1	1055	952	102.7
L3	986	860	126.5
L4	962	850	112.1
L5	939	766	172.6

Figure 61. Belt fit visualization using laser scan data and belt routing measured in the vehicle mockup.

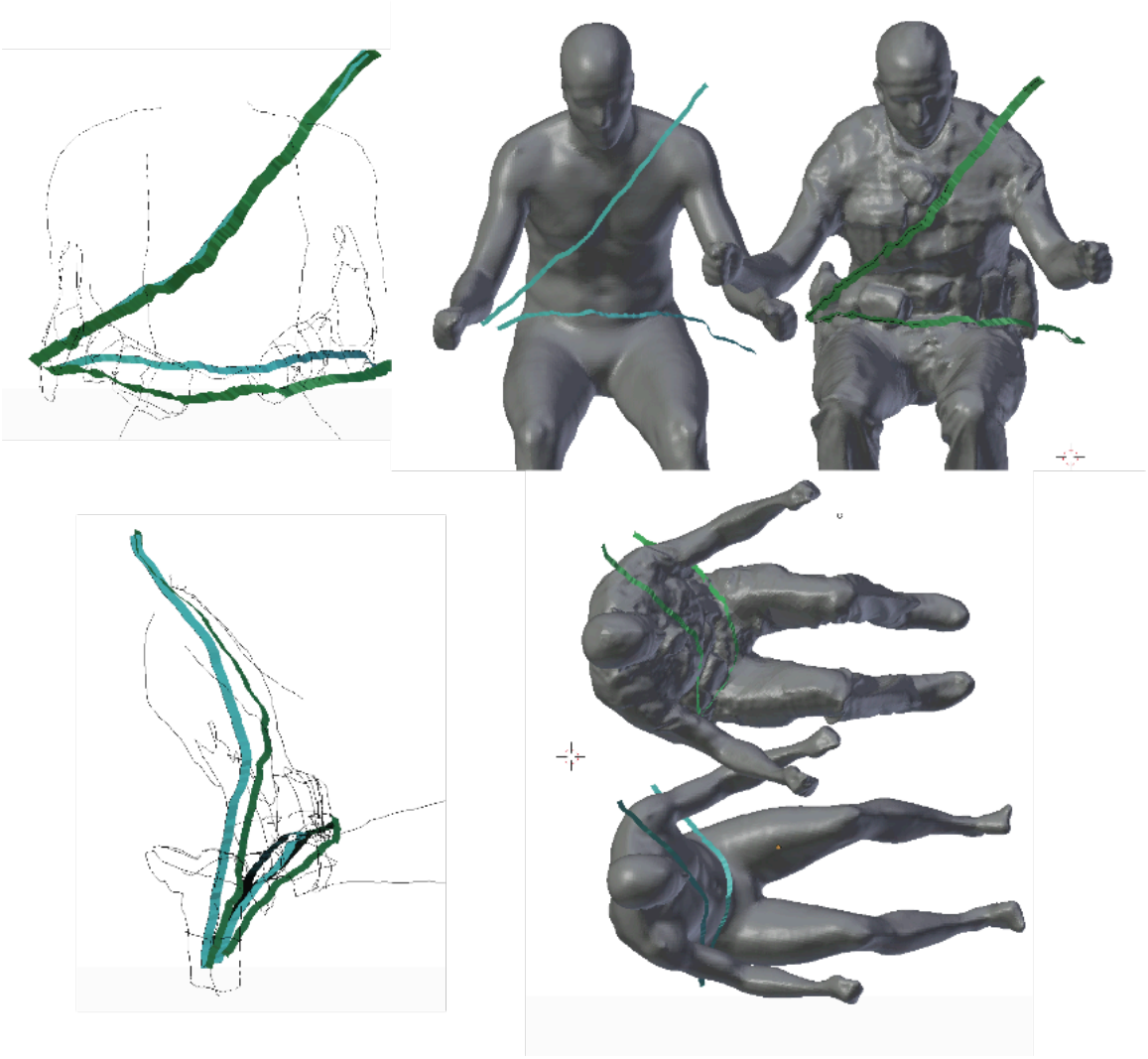

Figure 62. Belt fit visualization using laser scan data and belt routing measured in the vehicle mockup (blue – minimally clad; green – uniform).

4.5 Interaction with Seat and Vehicle Geometry

The measurement of officers in their vehicles demonstrated that interference between body-borne equipment is common and leads to disaccommodation and discomfort. Interference between seat back bolsters and the equipment on the duty belt was common, as was interference with the center console and door (Figure **63**-Figure **67**).

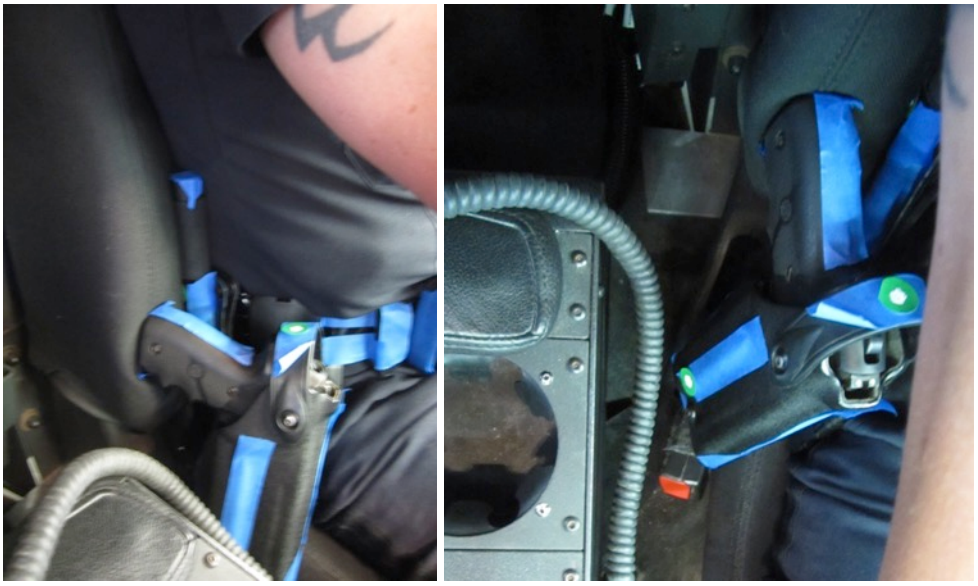

Figure 63. Interference between the duty belt and seatback bolster (left) and center console (right).

Figure 64. Radio digging into bolster (note seat wear due to equipment contact during ingress).

Figure 65. Officer showing interaction between thigh holster and center console (left), which makes donning the seat belt difficult. The belt then covers the weapon making it impossible to draw quickly. The scratch marks on center console from holster (right).

Figure 66. Female officer in Tahoe seat (L2). Officer reports interference of communication radio with seatback bolsters.

Figure 67. Interference between the duty belt and seatback bolster (L3).

4.6 Analysis of Seat Fit Using Scan Data

Data from laser scans of the equipped officers were combined with line-scan data from the seats to demonstrate a three-dimensional analysis of seat fit. Figure **68** and Figure **69** show seat and body data overlaid. With the current methods, the body scan postures do not exactly match the in-vehicle postures, but methods for adjusting the scan data to in-vehicle postures could be applied in future studies (Reed, 2013). With a larger sample of data, these 3D analyses could be used to develop seat design specifications that would accommodate a large percentage of officers and their gear while providing good support.

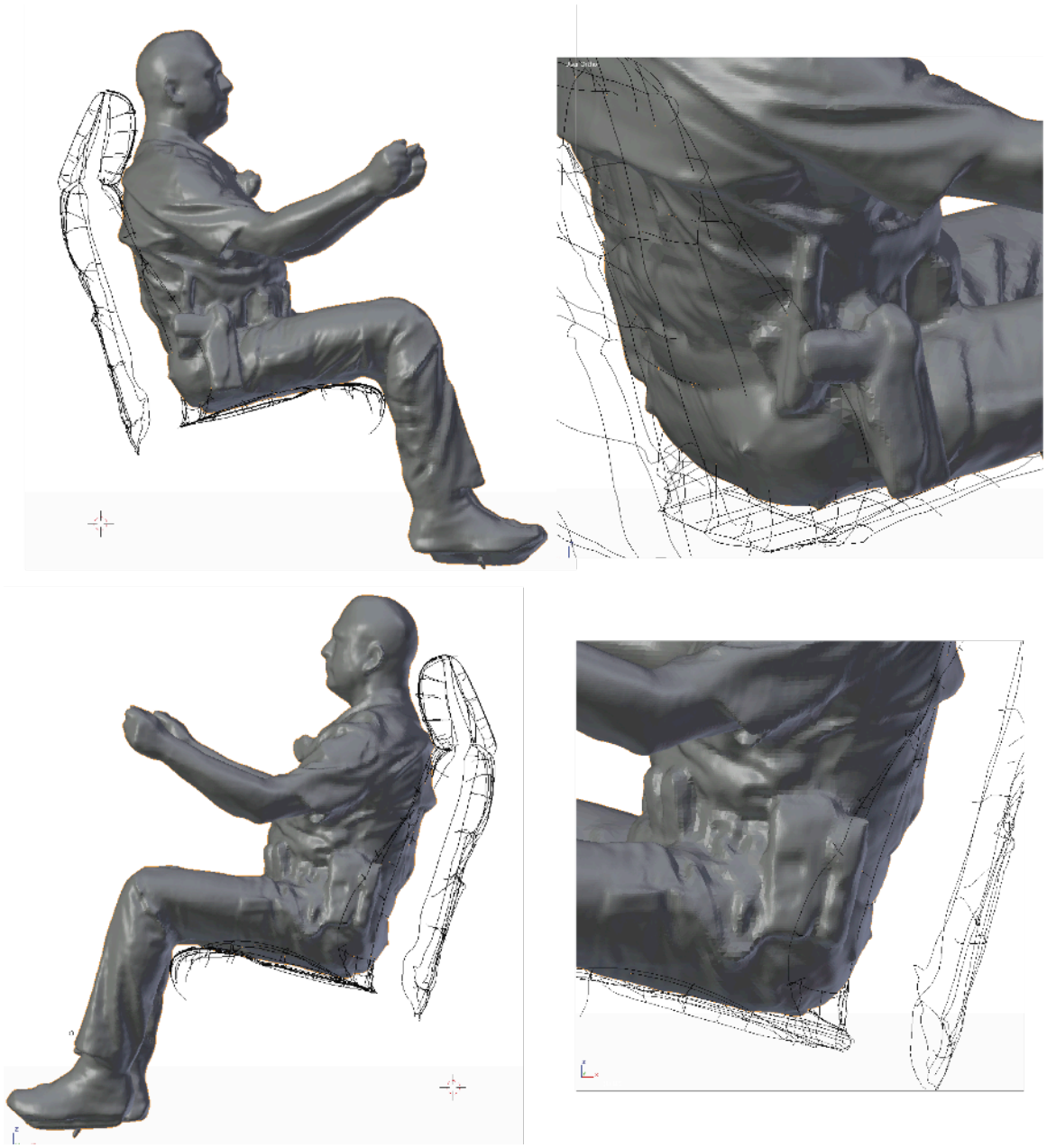

Figure 68. Duty belt interaction with seat back bolsters in a Ford Taurus seat (L5).

Figure 69. Side arm, flashlight, and mace create pressure point at lower back due to interaction with the seatback cushion and bolster in a Tahoe seat (L1).

4.7 In-vehicle Task Postures

Photographs were taken while officers demonstrated common in-vehicle tasks. As an example, Figure **70** illustrates the twisted spine and elevated shoulder postures required to use the center-mounted laptop computer.

Figure 70. In-vehicle task posture for using laptop computer.

5 Discussion

This pilot study demonstrated the use of three-dimensional functional anthropometry methods to quantify the interaction of the equipped LEO with vehicle interiors. The data included whole-body surface shape, landmark locations in driving postures, and safety belt routing relative to skeletal landmarks.

The pilot study results demonstrated substantial effects of body-borne equipment on LEO posture, position, and space claim. Although the current sample is too small to allow generalization to broader populations, some preliminary observations can be made:

- The duty belt, sidearm, and ballistic vest add substantially to the space requirements of the LEO, particularly in the waist, hip, and lumbar areas.

- The equipment on the duty belt interacts with the seat contour in disadvantageous ways, causing local discomfort, posture shifts that negate the effectiveness of the lumbar support, and difficulties with ingress and egress.

- The equipment on the duty belt and the sidearm often interfere with appropriate safety belt routing. The lap portion of the belt was frequently displaced from the preferred location close to the pelvis. For right-handed individuals, the sidearm holster on the duty belt was always observed to interfere with buckling of the belt. Officers reported that they may drive without the belt in situations in which they may need rapid access to their sidearms. Because belts are highly effective in preventing injury and fatality, the incompatibility between the belt and body-borne equipment increases the risks to officers.

- The vehicles examined in this study were adapted from general-purpose vehicles. The addition of barriers between the front and rear seats constrained the adjustability of the driver seat, such that larger officers were not able to obtain a comfortable posture. The officers reported a preference for certain vehicles that provided better accommodation. In no case, though, was the seat modified to provide appropriate relief for the equipment, nor were adaptations of the restraint systems observed.

- Modern police vehicles are mobile offices, with officers using laptop computers and communications systems. The postures for using the laptop invariably involve twisting of the spine and elevated shoulder angles. The long-term consequences of these postures may include lower-back, shoulder, and neck discomfort and injury.

This pilot study demonstrates that 3D functional anthropometry methods are effective in quantifying the interaction between LEOs and their vehicles. The preliminary results demonstrate a need for an expanded investigation in three areas:

1. quantifying the consequences of body-borne equipment on seated posture and developing seat designs that improve postural support and reduce discomfort for equipped officers,

2. quantifying the safety belt fit obtained by officers and developing alternative restraint designs that combine a high level of crash protection with comfort and compatibility with task performance requirements, and

3. quantifying the ergonomic stressors that result from current vehicle designs, including constraints on posture and motion as well as awkward task postures, and developing vehicle design procedures and guidelines that reduce or eliminate these limitations of current vehicles and ensure adequate accommodation for the officers.

We recommend that a large-scale study of LEO be conducted using the methods demonstrated in this pilot study. A sample of at least 100 male and female officers should be conducted, along with detailed measurements of common vehicle configurations. Restraint optimization studies should be conducted based on the analysis of data obtained from the officers, resulting in recommendations for new vehicle, seat, and restraint system designs.

References

Clarke, C., and Zak, M.J. (1999). *Fatalities to law enforcement officers and firefighters, 1992-1997, Compensation and Working Conditions*. U.S. Bureau of Labor Statistics.

Maguire, B.J., Hunting, K.L, Smith, G.S., and Levick, N.R. (2002). Occupational Fatalities in Emergency Medical Services: A Hidden Crisis. *Annals of Emergency Medicine*, 40(6): 625-632.

Oron-Gilad, T., Szalma, J.L., Stafford, S.C., and Hancock, P.A. (2005). Police officers seat belt use while on duty. *Transportation Research Part F* 8: 1-18.

Park, J., S.M. Ebert, M.P. Reed, & Hallman, J.J. (2015). Development of an optimization method for locating the pelvis in an automobile seat. *Proc. 4rd International Digital Human Modeling Conference*. Las Vegas, US.

Reed, M.P. (2013a). Modeling body shape from surface landmark configurations. *Human Modeling and Applications in Health, Safety, Ergonomics, and Risk Management. Human Body Modeling and Ergonomics. Lecture Notes in Computer Science,* 8026:376-383.

Reed, M.P., S.M. Ebert, & Hallman, J.J. (2013b). Effects of driver characteristics on seat belt fit. *Stapp Car Crash Journal*, 57, 43-57.

Reed, M.P., Ebert-Hamilton, S.M., Manary, M.A., Klinich, K.D., and Schneider, L.W. (2005). A new database of child anthropometry and seated posture for automotive safety applications. *SAE Transactions: Journal of Passenger Cars - Mechanical Systems*, 114: 2222-2235.

Reed,M.P.,Manary,M.A.,and Schneider, L.W. (1999). Methods for measuring and representing automobile occupant posture. Technical Paper 990959. *Society of Automotive Engineers*, Warrendale, PA.

Society of Automotive Engineers (SAE) J1100. (2009). Motor Vehicle Dimensions. Warrendale, PA: Society of Automotive Engineers, Inc.

Tiesman, H.M., Hendricks, S.A, Bell, J.L., and Harlan A. A. (2010). Eleven years of occupational mortality in law enforcement: the census of fatal occupational injuries, 1992–2002. *American Journal of Industrial Medicine,* 53:940–949.